doi.org/10.26434/chemrxiv.10119302.v1

A Sweet Galactose Transfer – Metabolic Oligosaccharide Engineering as a Tool to Study Glycans in Plasmodium Infection

Annabel Kitowski, Gonçalo Bernardes

Submitted date: 01/11/2019 • Posted date: 07/11/2019

Citation information: Kitowski, Annabel; Bernardes, Gonçalo (2019): A Sweet Galactose Transfer – Metabolic Oligosaccharide Engineering as a Tool to Study Glycans in Plasmodium Infection. ChemRxiv. Preprint. https://doi.org/10.26434/chemrxiv.10119302.v1

The use of artificial galactose derivatives and labelling through iEDDA reaction in the liver stage of Plasmodium infection showed increased uptake in infected hepatic cells, through participation of GLUT1 transporters. Furthermore, unprotected derivatives are transferred from the mosquito host to the Plasmodium berghei parasite. This strategy has the potential to provide new insights into Plasmodium glycobiology.

A sweet galactose transfer – Metabolic oligosaccharide engineering as a tool to study glycans in *Plasmodium* infection

Annabel Kitowski,[a] and Gonçalo J. L. Bernardes*[a,b]

[a] Instituto de Medicina Molecular João Lobo Antunes, Faculdade de Medicina, Universidade de Lisboa, Avenida Professor Egas Moniz, 1649–028 Lisboa (Portugal)

[b] Department of Chemistry, University of Cambridge, Lensfield Road, CB2 1EW Cambridge (UK)

Correspondence should be sent to: gb453@cam.ac.uk (G.J.L.B.) or gbernardes@medicina.ulisboa.pt (G.J.L.B.)

Abstract: The introduction of chemical reporter groups in glycan structures through metabolic oligosaccharide engineering (MOE) followed by bio-orthogonal ligation is an important tool to study glycosylation. We show the incorporation of synthetic galactose derivatives that bear terminal alkene groups in hepatic cells, with and without infection by *Plasmodium berghei* parasites, the causative agent of malaria. Additionally, we demonstrated the contribution of GLUT1 to the transport of these galactose derivatives, and observed moderate increase in the uptake of these compounds by *P. berghei*-infected cells, relative to their non-infected counterparts. Finally, we used MOE to study the interplay between *Plasmodium* parasites and their mosquito hosts, to reveal a possible transfer of galactose building blocks from the latter to the former. This strategy has the potential to provide new insights into *Plasmodium* glycobiology as well as for the identification and characterization of key glycan structures for further vaccine development.

Metabolic oligosaccharide engineering (MOE) is an important tool in carbohydrate research and chemical biology.[1] Next to proteins and nucleic acids, carbohydrates represent one of the largest groups of biomolecules, with a wide range of functionalities in health and disease states.[2] Although, for example, changes in protein structures can be addressed through the corresponding RNA sequence, carbohydrate structures are not template-encoded, which can complicate their investigation.[3] With the introduction of chemical reporter groups in glycan structures through MOE, new strategies have been developed to investigate glycan structures in different disease settings. Over the years, different synthetic monosaccharide derivatives of N-acetylmannosamine (ManNAc), N-acetylglucosamine (GlcNAc), sialic acid and N-acetylglucosamine (GalNAc) have been developed and used for MOE in different organisms and experimental settings.[4] However, to our knowledge, no examples of the use of galactose for MOE are presently available.

We decided to focus on the use of galactose, due to its apparent importance in the context of infection by *Plasmodium* parasites, the causative agents of malaria.[5] The glycobiology of *Plasmodium* parasites has been amply discussed and is the subject of several studies aimed at the identification of new drug targets or vaccine antigens.[6] Recent research suggest that the trisaccharide α-Gal and corresponding anti-α-Gal antibodies play an important role in the acquisition of immunity against malaria.[7] However, external factors are involved in the level of expression of these antibodies and it remains unclear how α-Gal is formed on the parasite.[7] During the course of a *Plasmodium* infection, sporozoites injected by an infected mosquito, travel in the blood stream from the initial injection site to the liver and invade hepatocytes. In fact, following a remarkable intrahepatic replication process, up to 40,000 merozoites are released from each infected hepatocyte, which initiates the symptomatic blood stage of infection.[8] This important feature of the liver stage of *Plasmodium* infection makes it a major target for the development of therapies and vaccines. It has been shown that *Plasmodium* sporozoite proteins, like the circumsporozoite protein (CSP), are presented by infected

hepatocytes during the liver stage and contribute, together with so far unidentified antigen structures, to the activation of $CD8^+$ T cells.[9] This observation, together with recent findings on the immunogenic properties of the α-Gal epitope, suggested the potential presence of galactose containing glycan structures on infected cells. To test this hypothesis, we decided to use synthetic galactose derivatives in combination with MOE to investigate different stages of *Plasmodium* infection.[7a]

Starting from commercially available 1,6-anhydro-3,4-isopropylidene-β-D-galactopyranose, three galactose derivatives with differently sized terminal–alkene reporter groups were synthesized (**Figure 1a**). The introduced chemical reporters were addressed after metabolic incorporation through inverse electron-demand Diels–Alder (iEDDA) reaction with 6-methyl-tetrazine compounds. Briefly, derivatives **2a**, **2b** and **5** were obtained through classical Williamson-ether synthesis, followed by deprotection and acetylation of the monosaccharide. Zémplen deacetlyation resulted in deprotected derivatives **3a**, **3b** and **6** (see SI). The determination of the second-order rate constants for these derivatives in the iEDDA reaction was conducted in 96-well-plates with a microplate reader, and the decrease in specific tetrazine absorbance at 530 nm was monitored. The measurements were performed at 37 ºC in PBS, pH = 7.4. After determining the pseudo-first–order rate constant k_{obs} at different concentrations, an exponential decay function was used to calculate the corresponding second-order–rate constants (**Figure S1**). In agreement with previous studies that used mannosamine derivatives, the longer pentenyl–substituted derivatives showed faster kinetics when reacted with 6-methyl-tetrazine-amine relative to the shorter allyl–substituted derivative (**Figure 1b**).[10]

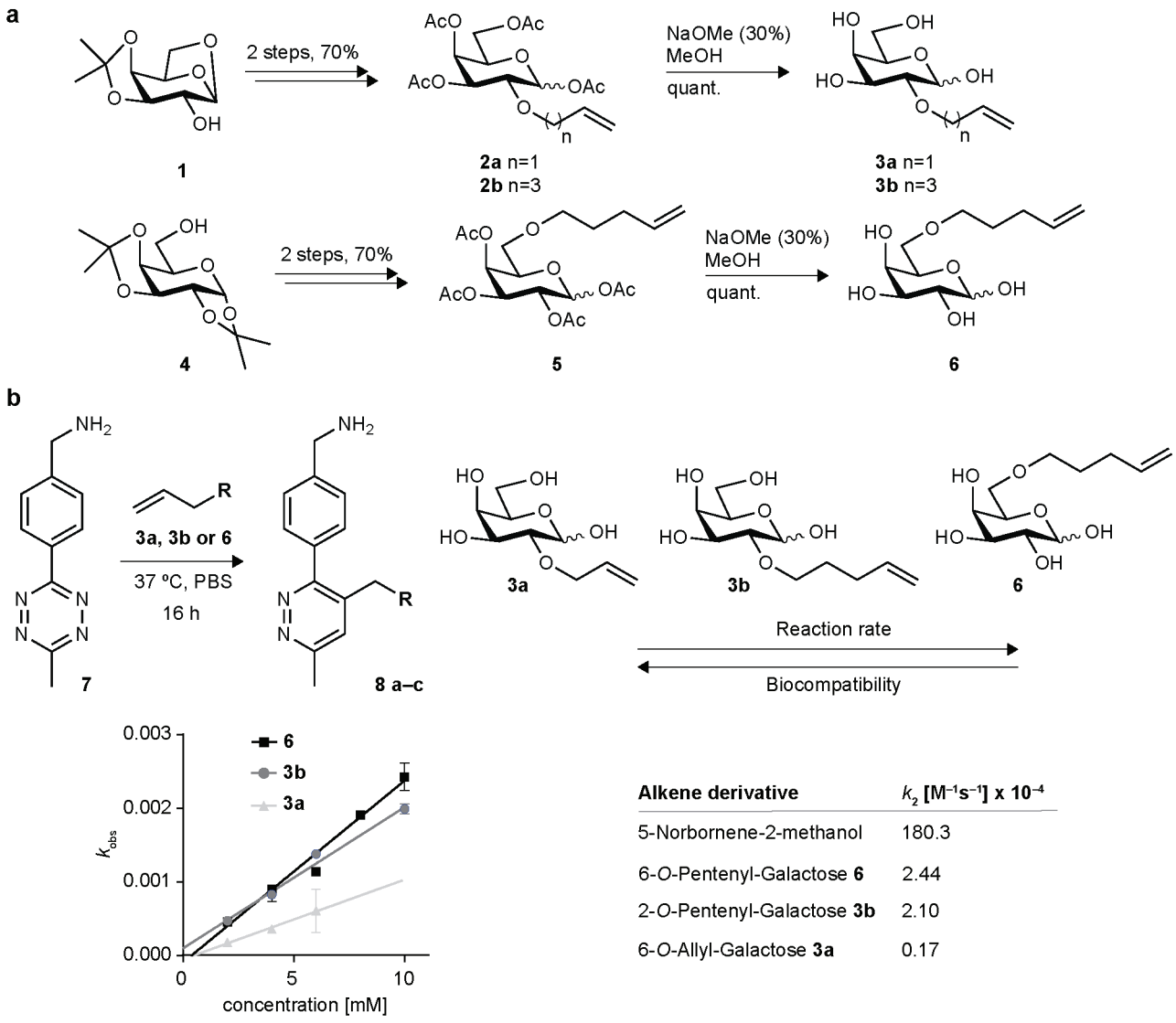

Alkene derivative	k_2 [$M^{-1}s^{-1}$] x 10^{-4}
5-Norbornene-2-methanol	180.3
6-*O*-Pentenyl-Galactose **6**	2.44
2-*O*-Pentenyl-Galactose **3b**	2.10
6-*O*-Allyl-Galactose **3a**	0.17

Figure 1. a. Synthesis of galactose derivatives **2a**, **2b**, **3a**, **3b**, **5** and **6** for metabolic labelling. **b.** Kinetic measurements and determination of the second order rate constant for iEDDA reaction between tetrazine **7** and monosaccharides **3a**, **3b** and **6**.

We started by employing these galactose derivatives to study the liver stage of a *Plasmodium* infection. Considering the importance of the α-Gal epitope for anti-malarial immunity, we sought to understand whether a change in galactose-containing glycans was observed on hepatocytes after infection with the *Plasmodium* parasite.[7b] To this end, we started by investigating the metabolic incorporation of the synthesized galactose derivatives into human hepatoma cells. In general, cells were grown for 48–72 h in the presence of 100 μM of **2a**, **2b**, **5** or natural

counterpart penta-*O*-acetyl-D-galactose **9**, before treatment with 6-methyl-tetrazine-PEG4-biotin, which served as a handle for further labelling (**Figure 2a**). All derivatives were non-toxic at the concentrations employed in the experiments (**Figure S2**). Huh7 and HepG2 cells were grown for 72 h in complete Dulbecco's Modified Eagle's medium, supplemented with 100 μM of the galactose derivatives **2a**, **2b**, **5** and control **9**, followed by labelling of the cell membrane with 6-methyl-tetrazine-PEG4-biotin, which served as an handle for further labelling, and Alexa-fluor-568-streptavidin (**Figure 2a**). Analysis and quantification of the fluorescence intensity was performed by using confocal point-scanning microscopy and ImageJ software. In compliance with the kinetic evaluations, a stronger fluorescence signal was detected for derivatives **2b** and **5** relative to **2a** (**Figure 2b** and **S3**). The marginal signal increase observed for derivative **5** relative to **2b** may be explained by the slightly higher kinetics of **5**, due to its lower steric hindrance, as a result of the presence of the pentenyl group in C6 instead of C2. Epimerization to glucose was excluded because no labelling was observed after treatment with β-galactosidase (**Figure 2c**). The incorporation of **2b** or **5** into glycoprotein structures was also corroborated in pull-down experiments (**Figure S11**). Additionally, competition experiments using **9** and benzyl 2-acetamido-2-deoxy-D-galactopyranoside confirmed the incorporation of **2b** also in *O*-glycans in addition to *N*-glycans (**Figure S12** and **S13**).

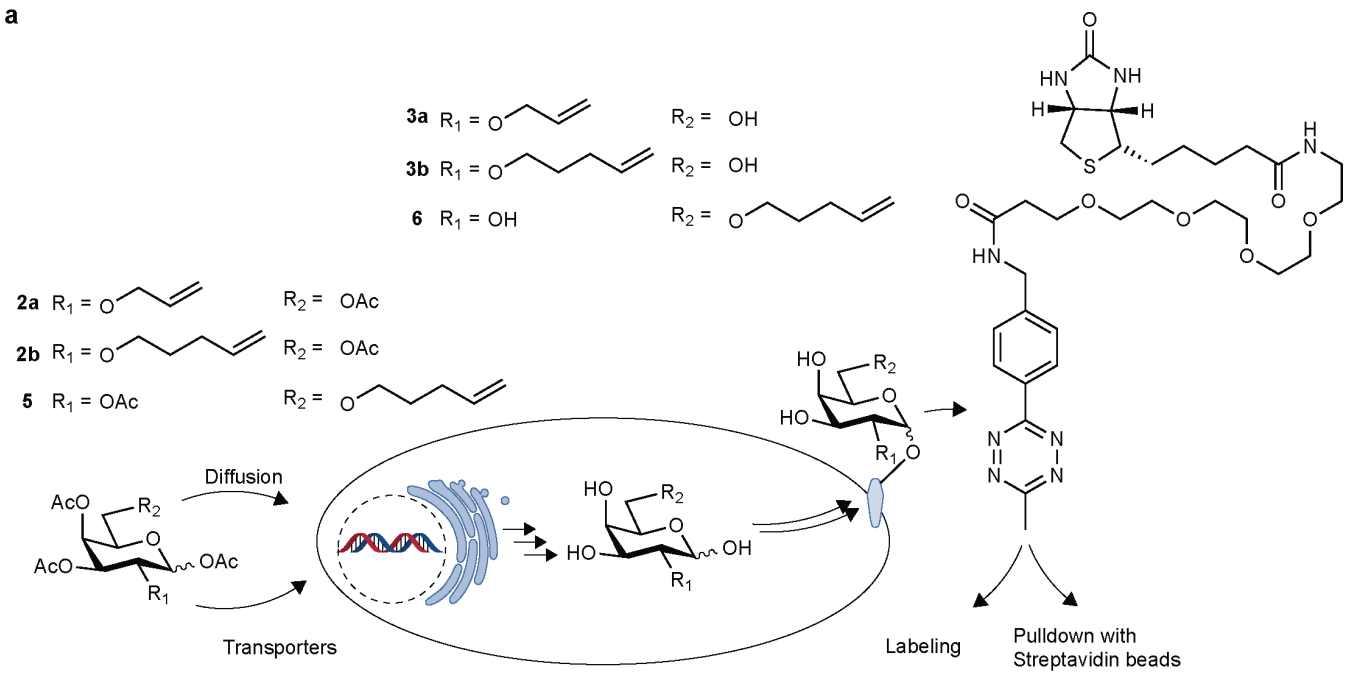
a
3a R1 = O R2 = OH
3b R1 = O R2 = OH
6 R1 = OH R2 = O
2a R1 = O R2 = OAc
2b R1 = O R2 = OAc
5 R1 = OAc R2 = O
Diffusion
Transporters
Labeling
Pulldown with Streptavidin beads

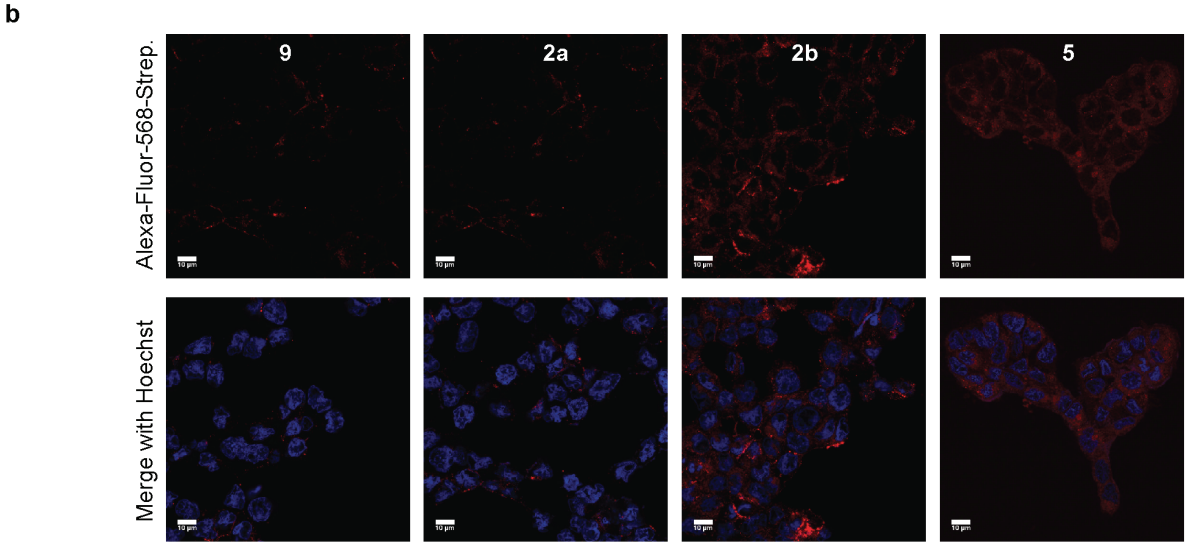
b
Alexa-Fluor-568-Strep.
Merge with Hoechst
9
2a
2b
5

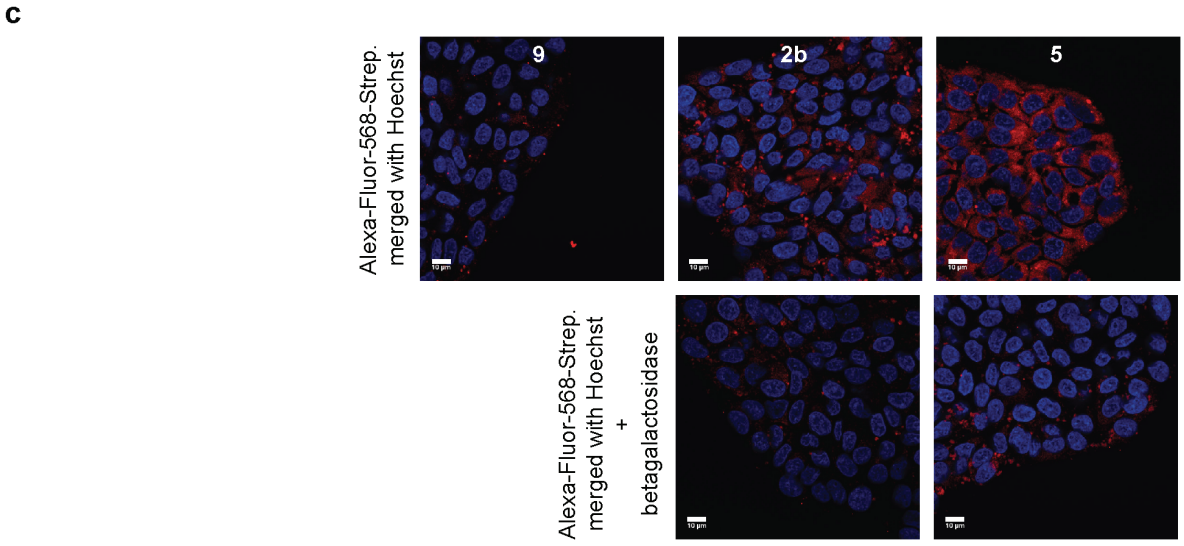
c
Alexa-Fluor-568-Strep. merged with Hoechst
Alexa-Fluor-568-Strep. merged with Hoechst + betagalactosidase
9
2b
5

Figure 2. a. Schematic description of the incorporation of galactose derivatives into cell–surface glycans and targeting strategies with 6-methyl-tetrazine-PEG4-biotin. **b.** Incorporation of **2a**, **2b**, and **5** in Huh7 cells, labelling with Alexa-Fluor-568-streptavidin (red) and Hoechst (blue) **c.** Incorporation of **2b, 5** and **9** in HepG2 cells and treatment with β-galactosidase (1U, 30 min, 37 ºC), labelling with Alexa-Fluor-568-streptavidin (red) and Hoechst (blue). Scale, 10 μm.

Chen and co-workers reported cysteine *S*-glycosylation by acetylated non-natural monosaccharides during MOE.[11] Thus, we decided to attempt the direct incorporation of non-acetylated derivative **3b** in glycans present in the cell membrane of HepG2 cells (**Figure S5**). Growing HepG2 cells for 72 h in presence of **3b** (100 μM) resulted in the successful incorporation of the unprotected galactose derivative, which could be fluorescently labelled by using our iEDDA approach. Our data suggests the incorporation of the galactose derivatives into the newly synthetized glycan structures rather than *S*-glycosylation.

Having shown the successful incorporation of the artificial galactose derivatives by human hepatic cells, we then sought to investigate how this incorporation might change in the context of the liver stage of *Plasmodium* infection. To this end, HepG2 cells were infected with GFP-expressing *P. berghei* sporozoites freshly isolated from salivary glands of infected *Anopheles* mosquitoes, and the cells were grown in the presence of 100 μM of **2b** or **9** until 48 h post-infection (hpi). Galactose incorporation was analyzed by confocal point-scanning microscopy and imaging flow cytometry (**Figure 3a**). Confocal point-scanning microscopy showed a clear labelling of the glycans in the cell membrane, both in non-infected and in *P. berghei*-infected cells (**Figure 3b**). The incorporation of **2b** was then analyzed by imaging flow cytometry 48 h after sporozoite addition, which allows distinguishing, infected cells, containing the GFP-expressing parasite, from non-infected cells (**Figure S6**). To answer our question regarding the change of galactose-containing glycans in *P. berghei*-infected hepatocytes, we performed our MOE strategy using iEDDA reaction with 6-methyl-tetrazine-PEG4-biotin and subsequent

labelling with Alexa-Fluor-568-streptavidin. Analyzing this signal indicated a slight increase in uptake and incorporation of **2b** by hepatocytes which got infected by *P. berghei* sporozoites when compared to naïve hepatocytes (**Figure 3c**), although this effect was not statistically significant.

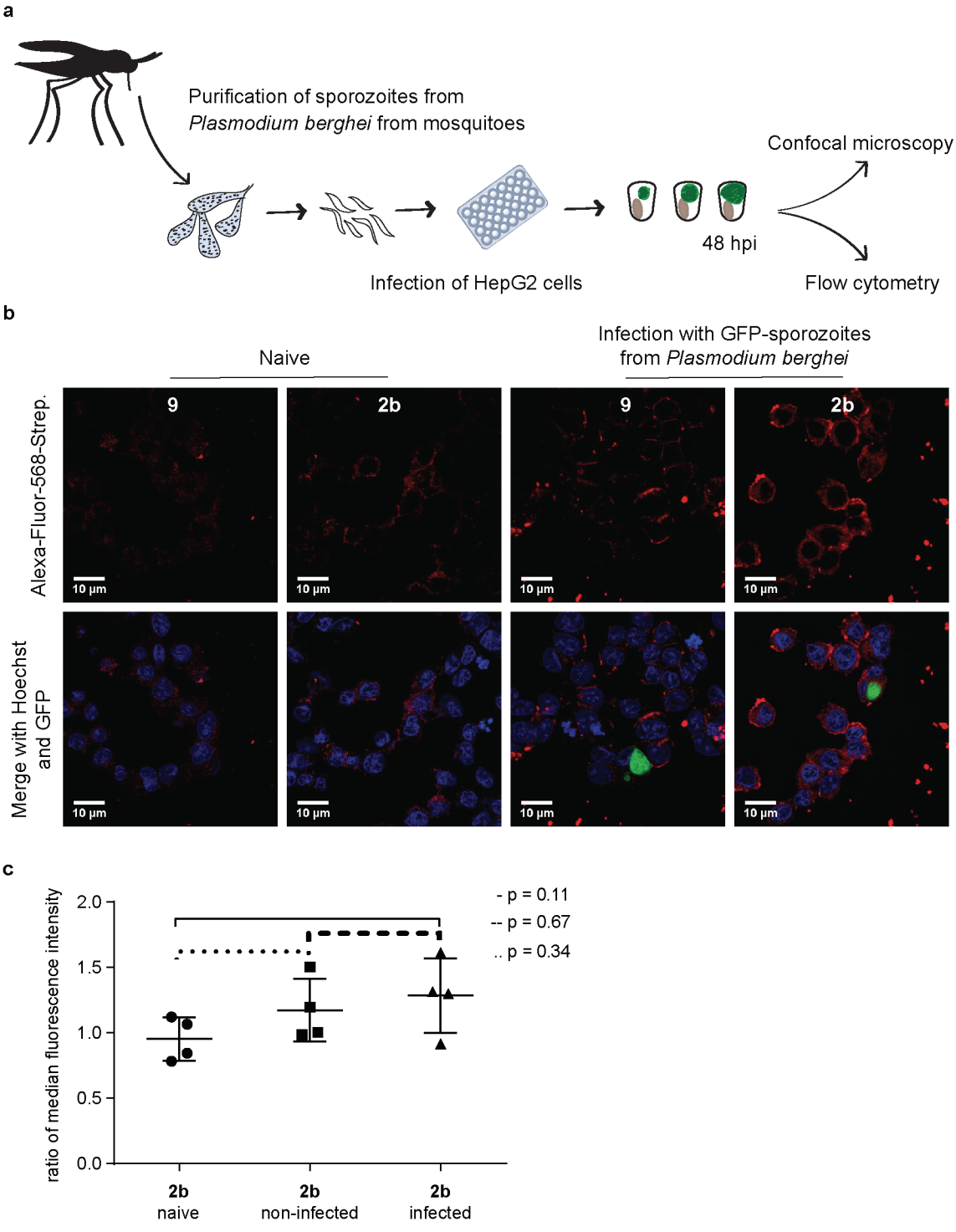

Figure 3. a. Workflow for the infection of HepG2 cells with sporozoites from *Plasmodium berghei* and metabolic incorporation of **2b**. **b.** Metabolic labelling of HepG2 cells with **2b** or **9** after infection with GFP-sporozoites from *Plasmodium berghei* (green), labelling with Alexa-Fluor-568-streptavidin (red) and Hoechst (blue) 48 hpi. **c.** Ratio of median fluorescence intensity from Alexa-Fluor-568-streptavidin of naïve, non-infected and infected HepG2 cells, acquired in Amnis ImageStreamX, ratio against corresponding control with **9**, pooled data of four individual experiments, each data point represents the median fluorescence intensity of 80 (infected) or 2000 cells (naïve, non-infected), two-tailed Mann-Whitney. Scale, 10 μm.

The observation of a moderate increase of incorporated galactose derivative **2b**, could suggest a change in certain metabolic events in *P. berghei*-infected hepatocytes. We started to look into metabolic hallmarks, which are known to occur during the course of parasite development in the infected hepatic cell, specifically the importance of hexose transporters for processes related to the energy metabolism of the developing parasite. It has been shown that, during the blood stage of *Plasmodium* infection, glucose is transported through GLUT1 into erythrocytes and taken up by the parasite by a facilitative hexose transporter (PfHT).[12] GLUT1 is also expressed in liver cells and it has been shown that the enhanced translocation of this transporter to the membrane of *P. berghei*-infected hepatic cells, leads to increased glucose uptake during the later stages of *Plasmodium* liver infection.[13] GLUT1 belongs to a family of class I facilitative glucose transporters, which also facilitates the diffusion of galactose.[14] We hypothesized that the moderate increase observed in the uptake of galactose derivative **2b** by infected cells, could be related with the reported increased translocation of GLUT1 to the cell membrane of those cells. In this case, our artificial galactose derivative **2b** would also be transported through the GLUT1 transporter. To test this hypothesis, we selected two specific GLUT1 inhibitors, WZB117 **10** and STF31 **11**, as well as non-specific inhibitor cytochalasin B **12** to block this transporter during the period of incubation with galactose derivative **2b** (**Figure**

4a). Briefly, HepG2 cells were grown as before in the presence of **2b** (100 μM) for 72 h, in the presence of 10 μM of each inhibitors **10**, **11** or **12**. Interestingly, a decrease in fluorescence intensity was observed in the presence of all the inhibitors employed, and a dose-dependent decline in fluorescence intensity in the presence of the selective inhibitor **10** (**Figure 4b**, **4c** and **S8**). These results confirm the ability of GLUT1 to transport artificial galactose structures into the cytosol. These results further support the notion that *P. berghei*-infected hepatic cells may take up more of derivative **2b**, due to the increased translocation of GLUT1 transporters to the cell membrane of these cells.

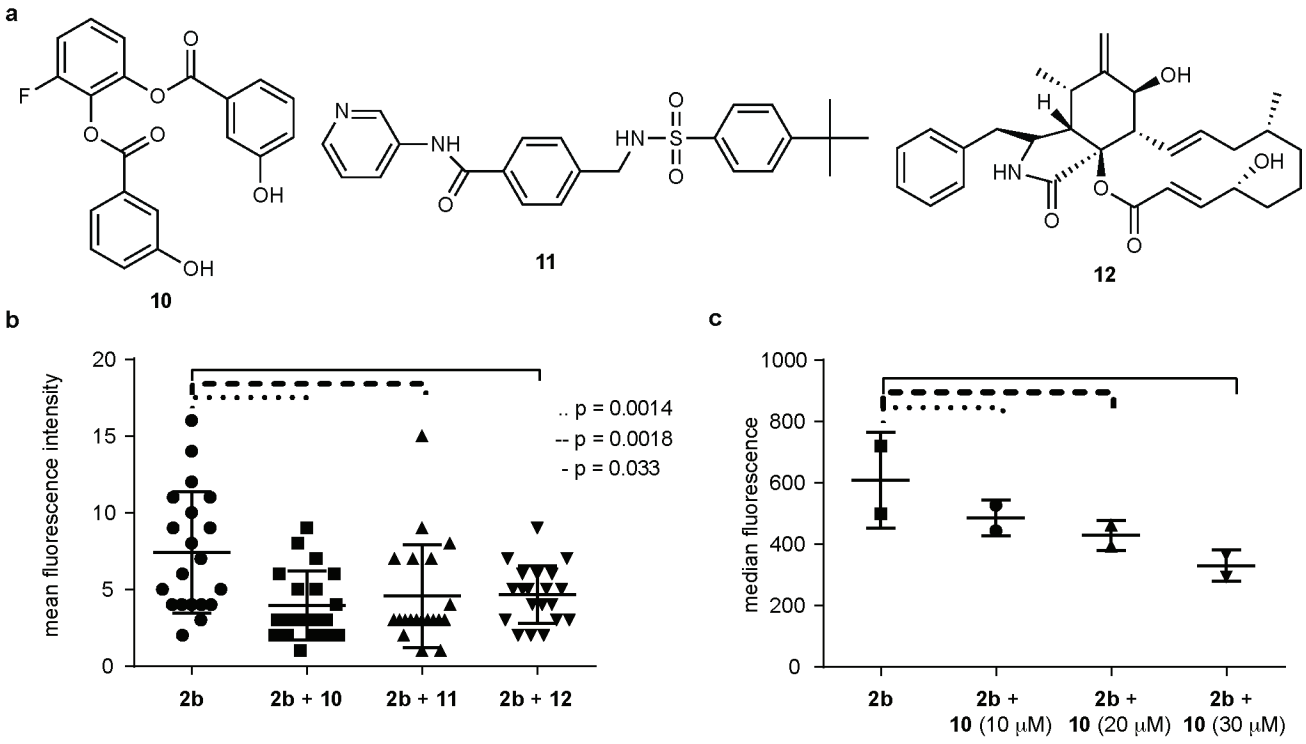

Figure 4. a. GLUT1 inhibitors WZB117 **10**, STF31 **11** and cytochalasine B **12**. **b.** Mean fluorescence intensity after metabolic incorporation of **2b** in the presence of 10 μM of inhibitors **10**, **11** and **12**. Two-tailed Mann-Whitney **c.** Concentration-dependent decrease in fluorescence intensity after metabolic incorporation of **2b** with increasing concentration of inhibitor **10**, pool of two independent experiments, two-tailed Mann-Whitney.

Having employed artificial galactose derivatives to investigate galactose uptake by *Plasmodium*-infected hepatic cells, we then sought to extend our MOE approach to the study of the *Plasmodium* parasite itself. As previously mentioned, the presence of IgM antibodies against the trisaccharide α-Gal was reported to provide a protective effect against malaria transmission.[7a] Although the α-Gal epitope has been detected on sporozoites from *P. falciparum*, *P. berghei* and *P. yoelii*, the enzymes required for assembly of this epitope have not yet been identified.[6a, 7a] Residual levels of this epitope were also detected in proteins from salivary glands of non-infected *Anopheles* mosquitoes, which could suggest a transfer of substrates or structures from the mosquito host to the parasite.[7a] We therefore employed our MOE strategy to test this hypothesis and assess a possible transfer of administered galactose compounds from *Anopheles* mosquitoes to *Plasmodium* parasites. To this end, female *A. stephensi* mosquitoes were fed with a sugar solution, supplemented with either **2b** or its deprotected counterpart **3b**. Pentaacetylated galactose **9** or galactose **13** were used as negative controls in these experiments. The feeding was initiated after the mosquitoes' infectious blood meal and was maintained for 21–24 days. After this period, mosquito salivary glands were collected and *P. berghei* sporozoites were isolated and analyzed by imaging flow cytometry (**Figure 5a**). Our results show that the fluorescence intensity, which corresponds to the incorporated galactose derivatives **2b** or **3b**, was significantly higher in sporozoites dissected from mosquitoes fed on deprotected galactose derivative **3b**, than that observed in sporozoites obtained from control mosquitoes. Thus, although the acetylated galactose derivative **2b** seemed not to be transferred from the mosquito to the parasite, our labelling approach by means of iEDDA reaction indicated the transfer of derivative **3b** (**Figure 5b**). This observed transfer of galactose molecules from the mosquito host to the *Plasmodium* parasite could explain the reported detections of α-Gal epitopes on the parasite surface. Interestingly, the sporozoites obtained from mosquitoes fed on derivative **3b**, seem to be slightly bigger in size than

sporozoites obtained from the control mosquitoes, whereas a smaller number of parasites was observed in the former than in the latter (**Figures S9** and **S10**).

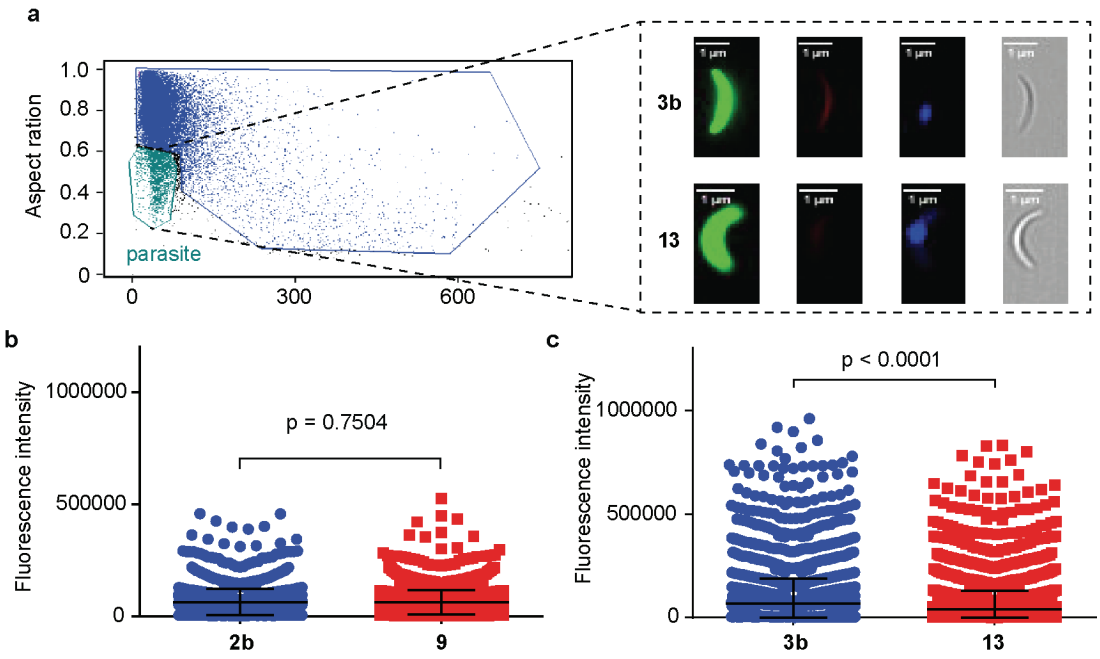

Figure 5. a. Gating strategy for acquisition of *Plasmodium berghei* sporozoites after incorporation of **3b**. Scale, 1 μm. **b.** Comparison of fluorescence intensity after labelling of sporozoites with 6-methyl-tetrazine-sulfo-Cy3, after incorporation of galactose derivative **2b** or control **9**. Two-tailed Mann-Whitney. **c.** Comparison of fluorescence intensity after labelling of sporozoites with 6-methyl-tetrazine-sulfo-Cy3, after incorporation of galactose derivative **3b** or control **13**. Two-tailed Mann-Whitney.

This proof-of-concept study demonstrates the application of MOE with artificial galactose derivatives in the context of *Plasmodium* infection. We showed the participation of GLUT1 transporters in the facilitated diffusion of the artificial galactose derivatives and a moderate enhancement in the amount of galactose derivative incorporated in *P. berghei*-infected hepatic cells relative to that observed in naïve cells. We further employed the MOE approach to demonstrate the transfer of the artificial galactose derivative **3b** from the mosquito host to the parasite. The impact of the introduction of an artificial sugar structure on the quality and

infectivity of the sporozoites requires further investigation. In summary, the approach presented in this study demonstrates the usefulness of MOE for further investigations on the *Plasmodium* glycobiology and might open new possibilities for the identification and characterization of important glycan structures for vaccine development.

Acknowledgements

Funded under the Marie Skłodowska-Curie ITN GA No. 675671, the Royal Society (URF\R\180019 to G.J.L.B.) and FCT Portugal (iFCT IF/00624/2015 to G.J.L.B.). We also thank Drs. Miguel Prudêncio and Vanessa Zuzarte-Luís for useful comments, and Dr. Vikki Cantrill for her help with the editing of this manuscript.

[1] a) P.-A. Gilormini, A. R. Batt, M. R. Pratt, C. Biot, *Chem. Sci.* **2018**, *9*, 7585–7595; b) S. T. Laughlin, C. R. Bertozzi, *Proc. Natl. Acad. Sci. USA* **2009**, *106*, 12–17.

[2] a) K. Ohtsubo, J. D. Marth, *Cell* **2006**, *126*, 855–867; b) D. H. Dube, C. R. Bertozzi, *Nat. Rev. Drug Discov.* **2005**, *4*, 477–488.

[3] P. H. Seeberger, D. B. Werz, *Nature* **2007**, *446*, 1046–1051.

[4] a) B. Cheng, R. Xie, L. Dong, X. Chen, *ChemBioChem* **2016**, *17*, 11–27; b) T. J. Sminia, H. Zuilhof, T. Wennekes, *Carbohydr. Res.* **2016**, *435*, 121–141.

[5] a) R. Ramasamy, R. T. Reese, *Mol. Biochem. Parasitol.* **1986**, *19*, 91–101; b) M. von Itzstein, M. Plebanski, B. M. Cooke, R. L. Coppel, *Trends Parasitol.* **2008**, *24*, 210–218.

[6] a) M. Cova, J. A. Rodrigues, T. K. Smith, L. Izquierdo, *Malar. J.* **2015**, *14*, 427; b) J. A. Jaurigue, P. H. Seeberger, *Front. Cell. Infect. Microbiol.* **2017**, *7*, 248–248.

[7] a) B. Yilmaz, S. Portugal, Tuan M. Tran, R. Gozzelino, S. Ramos, J. Gomes, A. Regalado, Peter J. Cowan, Anthony J. F. d'Apice, Anita S. Chong, Ogobara K. Doumbo, B. Traore, Peter D. Crompton, H. Silveira, Miguel P. Soares, *Cell* **2014**, *159*, 1277–1289; b) R. Aguilar, I. Ubillos, M. Vidal, N. Balanza, N. Crespo, A. Jiménez, A. Nhabomba, C. Jairoce, D. Dosoo,

B. Gyan, A. Ayestaran, H. Sanz, J. J. Campo, G. P. Gómez-Pérez, L. Izquierdo, C. Dobaño, *Sci. Rep.* **2018**, *8*, 9999.

[8] A. F. Cowman, J. Healer, D. Marapana, K. Marsh, *Cell* **2016**, *167*, 610–624.

[9] a) P. Bertolino, D. G. Bowen, *Front. Microbiol.* **2015**, *6*, 41; b) I. A. Cockburn, R. Amino, R. K. Kelemen, S. C. Kuo, S.-W. Tse, A. Radtke, L. Mac-Daniel, V. V. Ganusov, F. Zavala, R. Ménard, *Proc. Natl. Acad. Sci. USA* **2013**, *110*, 9090–9095.

[10] A.-K. Späte, V. F. Schart, S. Schöllkopf, A. Niederwieser, V. Wittmann, *Chem. Eur. J.* **2014**, *20*, 16411–16411.

[11] W. Qin, K. Qin, X. Fan, L. Peng, W. Hong, Y. Zhu, P. Lv, Y. Du, R. Huang, M. Han, B. Cheng, Y. Liu, W. Zhou, C. Wang, X. Chen, *Angew. Chem. Int. Ed.* **2018**, *57*, 1817–1820.

[12] C. J. Woodrow, R. J. Burchmore, S. Krishna, *Proc. Natl. Acad. Sci. USA* **2000**, *97*, 9931–9936.

[13] P. Meireles, J. Sales-Dias, C. M. Andrade, J. Mello-Vieira, L. Mancio-Silva, J. P. Simas, H. M. Staines, M. Prudêncio, *Cell. Microbiol.* **2017**, *19*, e12646.

[14] A. Carruthers, J. DeZutter, A. Ganguly, S. U. Devaskar, *Am. J. Physiol. Endocrinol. Metab.* **2009**, *297*, E836–E848.

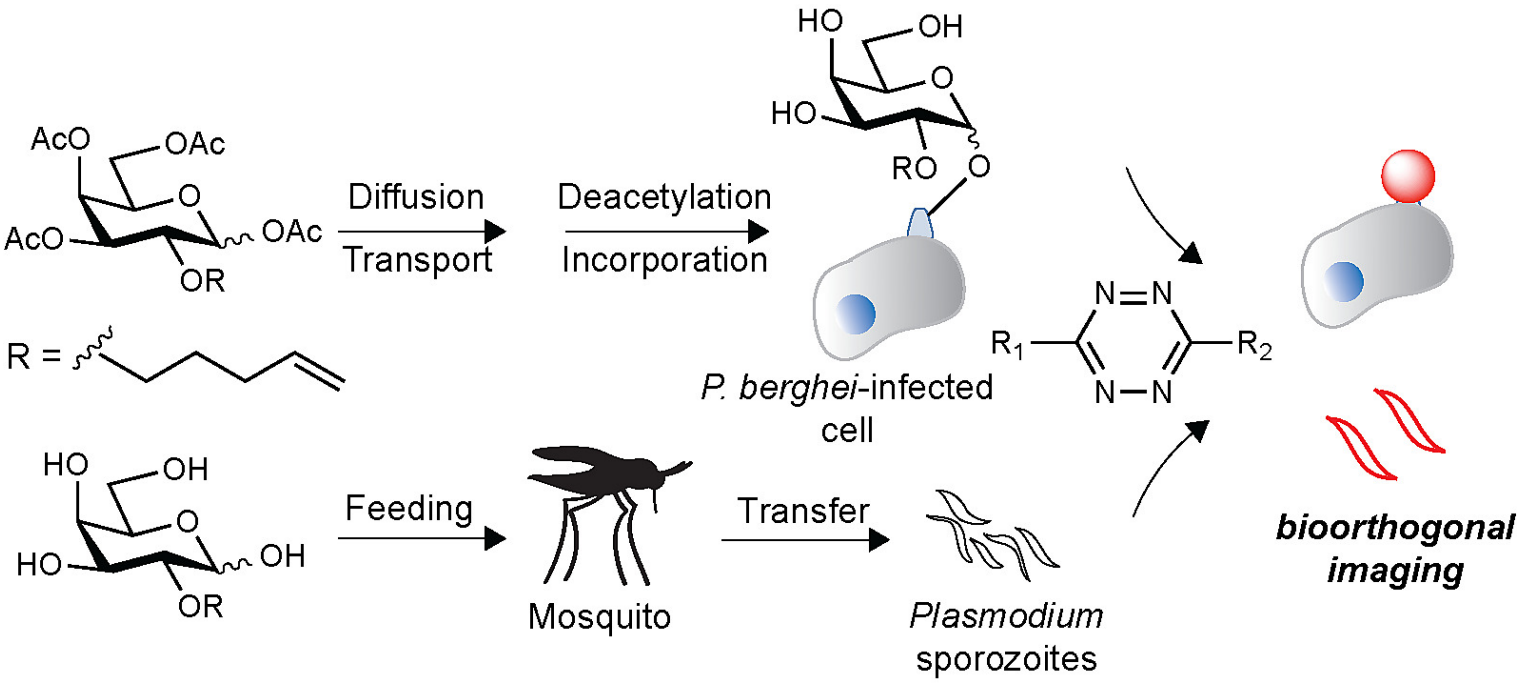

TOC.png (35.70 KiB)

view on ChemRxiv • download file

Supporting Information

Table of Contents

1. Supporting Figures

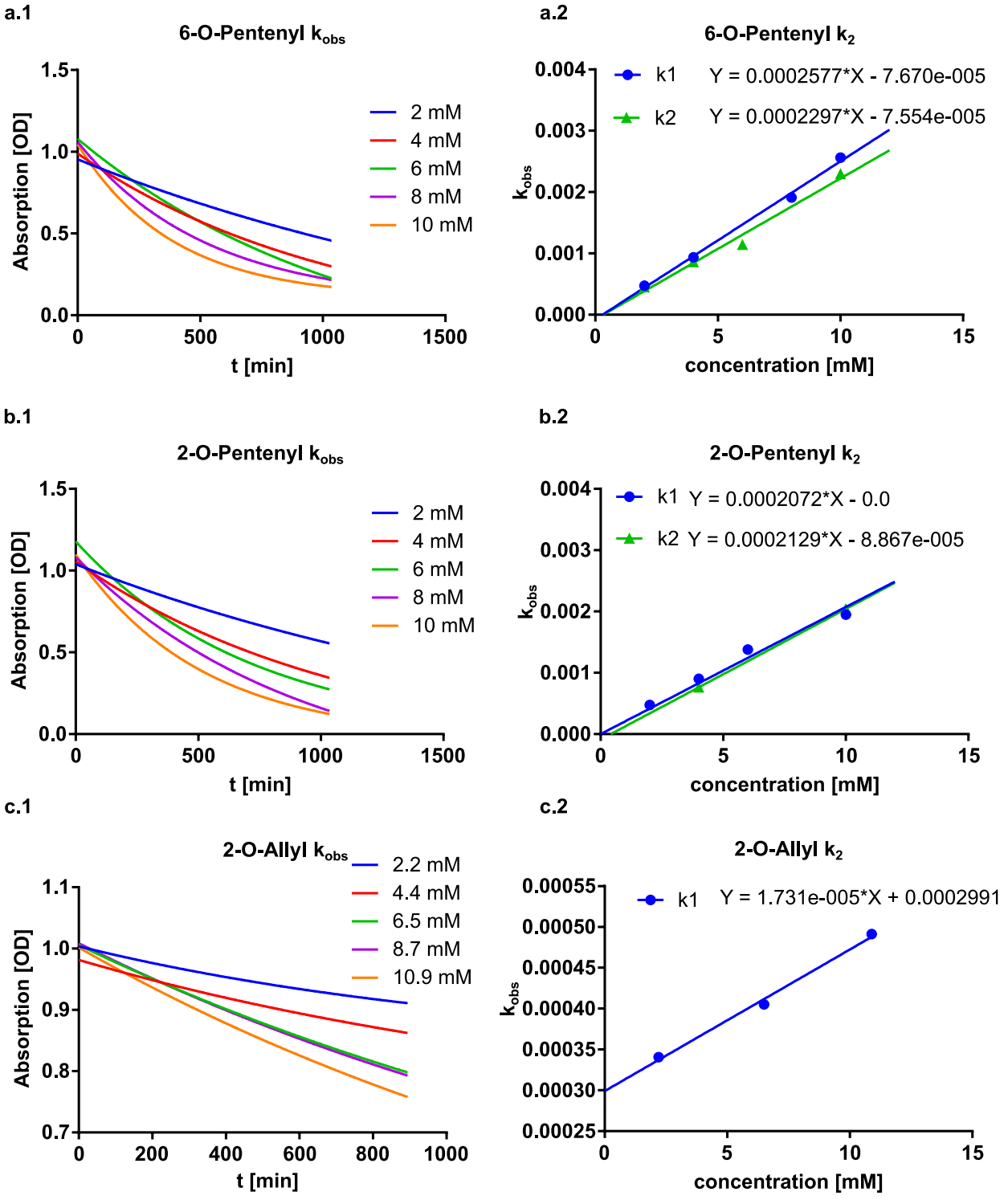

Figure S1: **a.1.** Decrease in absorbance of absorbance of 6-Methyl-tetrazine-amine at 530 nm with increasing concentrations of 6-O-Pentenyl-galactose in PBS pH = 7.4 at 37 °C. **a.2.** Plot of k_{obs} vs. the corresponding concentration of 6-O-Pentenyl-galactose **b.1.** Decrease in absorbance of absorbance of 6-Methyl-tetrazine-amine at 530 nm with increasing concentrations of 2-O-Pentenyl-galactose in PBS pH = 7.4 at 37 °C. **b.2.** Plot of k_{obs} vs. the corresponding concentration of 2-O-Pentenyl-galactose **c.1.**

Decrease in absorbance of absorbance of 6-Methyl-tetrazine-amine at 530 nm with increasing concentrations of 2-O-Allyl-galactose in PBS pH = 7.4 at 37 °C. **c.2.** Plot of k_{obs} vs. the corresponding concentration of 2-O-Allyl-galactose.

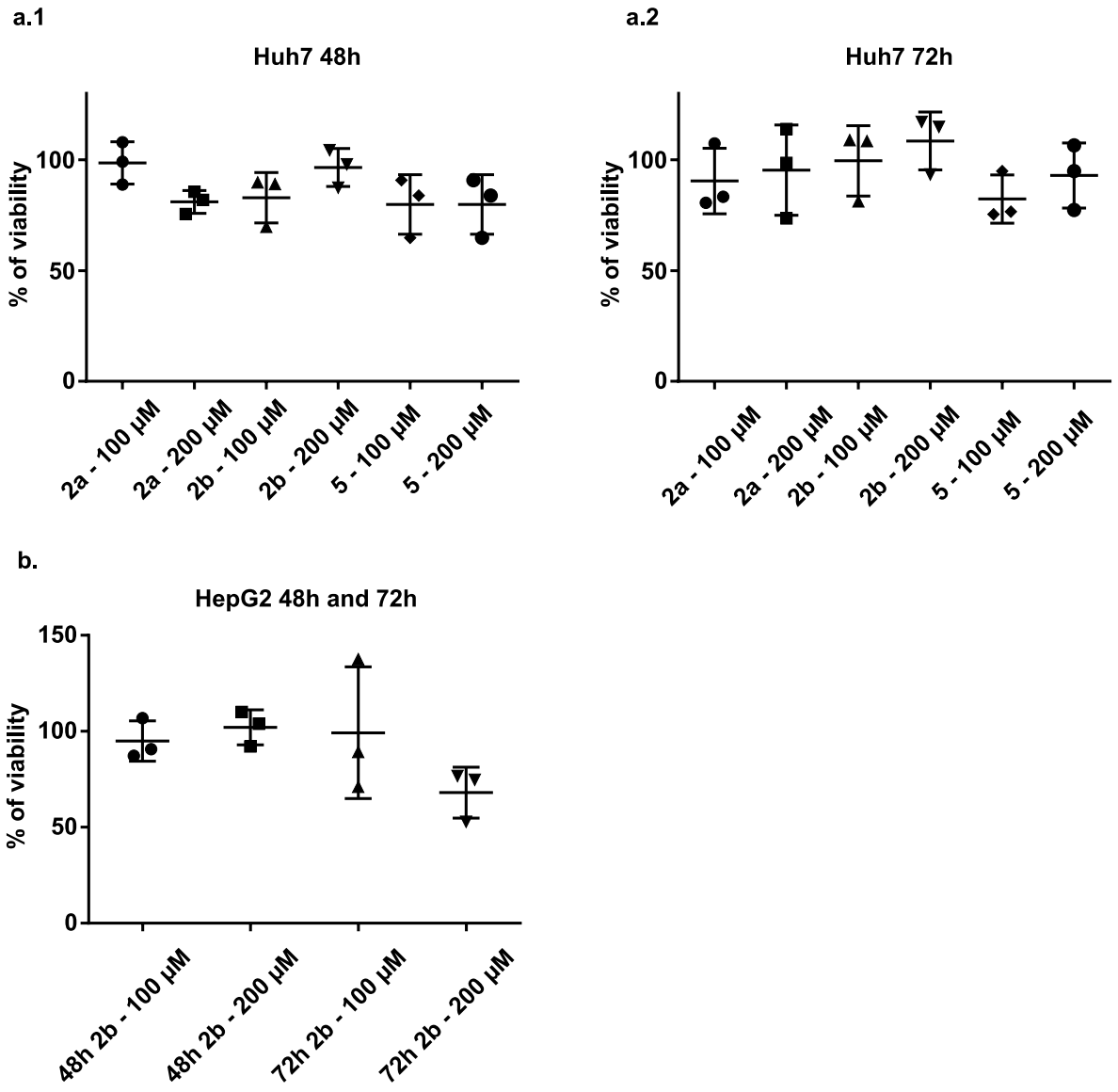

Figure S2: **a.1.** Viability of Huh7 cells incubated with artificial galactose derivatives for 48h, illustrated as percentage of maximum **a.2.** Viability of Huh7 cells incubated with artificial galactose derivatives for 72h, illustrated as percentage of maximum **b.** Viability of HepG2 cells incubated with artificial galactose derivatives for 48h and 72h, illustrated as percentage of maximum. Combined data from three independent experiments.

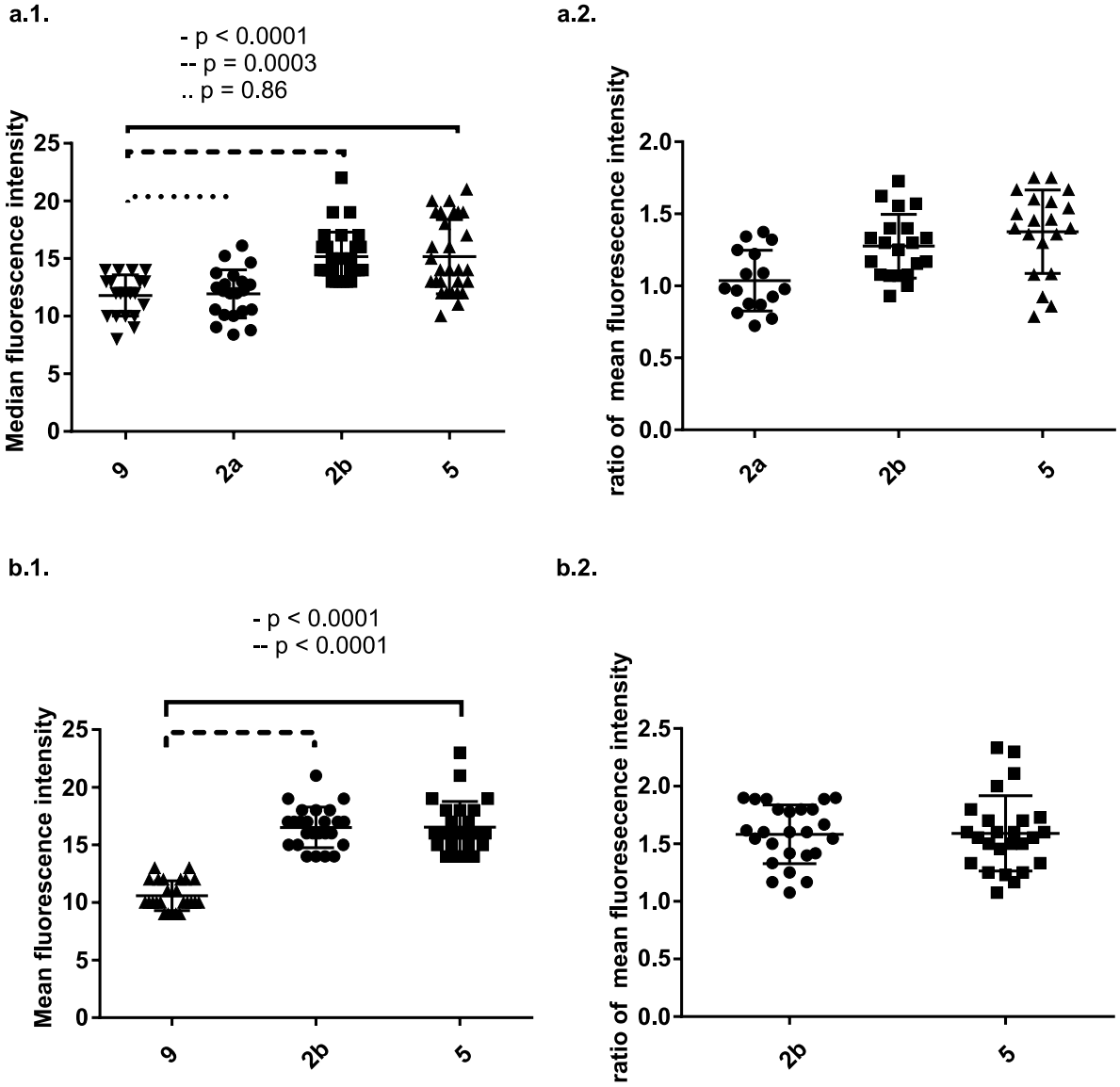

Figure S3: a.1. Quantification of Mean fluorescence intensity by confocal point-scanning micoroscopy after metabolic incorporation of **2a**, **2b** and **5** into cell membrane glycans of Huh7 cells, **9** was used as negative control. **a.2.** Ratio of mean fluorescence intensity against control **9** after metabolic incorporation of **2a**, **2b** and **5** in Huh7 cells. **b.2.** Quantification of Mean fluorescence intensity by confocal point-scanning microscopy after metabolic incorporation of **2b** and **5** into cell membrane glycans of HepG2 cells, **9** was used as a negative control. **b.2.** Ratio of mean fluorescence intensity against control **9** after metabolic incorporation of **2b** and **5** in HepG2 cells. Representative data from one out of three experiments, analysis of five to six picture per condition and 5-6 cells per picture, Two-tailed Mann-Whitney for non-parametric distribution, D'Agostino and Pearson omnibus normality test was performed for each data set.

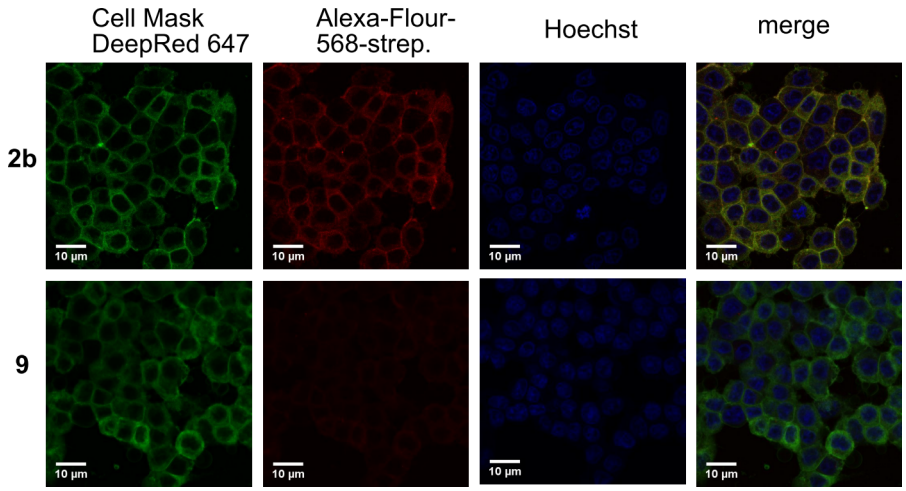

Figure S4: Metabolic incorporation of **2b** into HepG2 cells, labeling with 6-methyl-tetrazine-PEG4-biotin and Alexa-Flour-568-streptavidin (red). Co-staining of the cell membrane with CellMask Deep Red Plasma membrane stain (green). Nuclei were stained with Hoechst 33342, **9** was used as negative control.

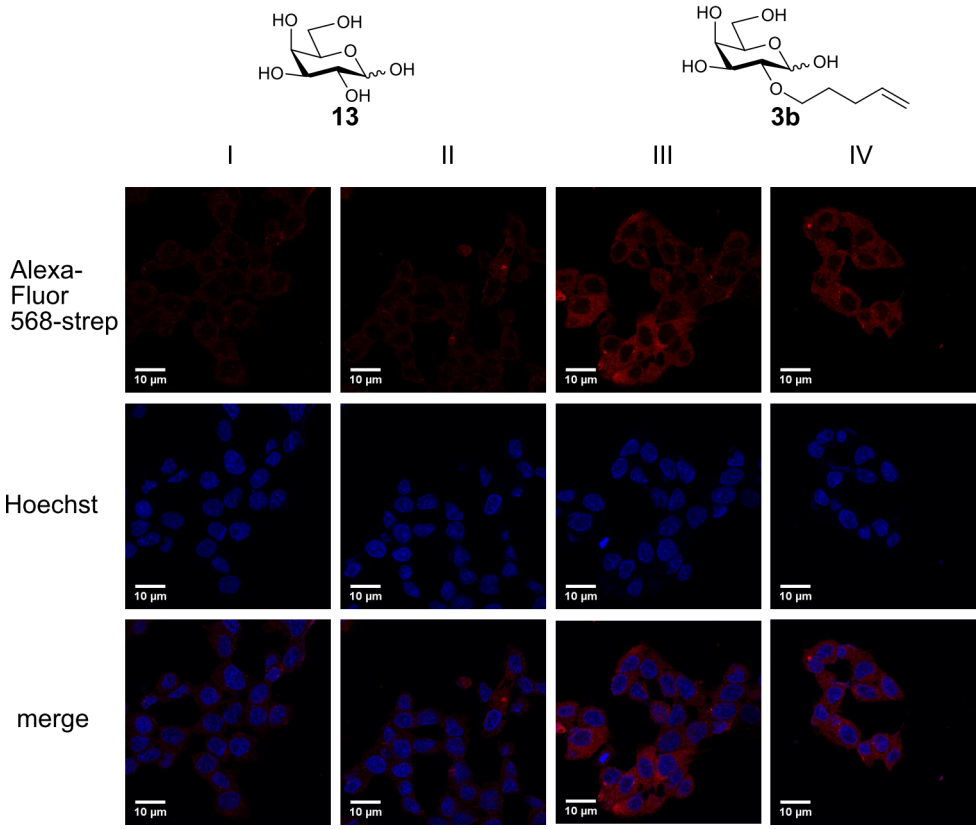

Figure S5: Incorporation of **13** and **3b** in HepG2 cells, labelling with Alexa-Fluor-568-streptavidin (red) and Hoechst (blue). I and III, as well as II and IV represent two independent experiments.

a.1

2b
no infection

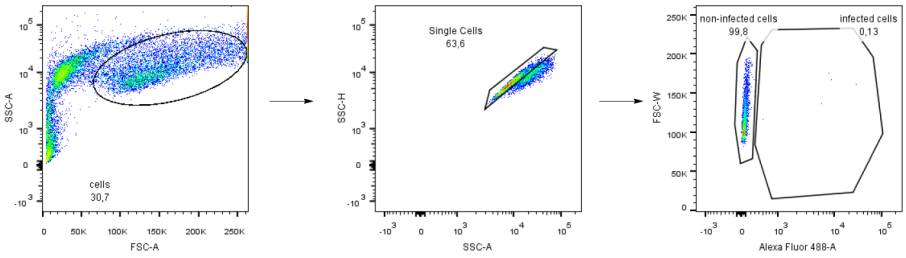

a.2

2b
infected with sporozoites from *P. berghei*

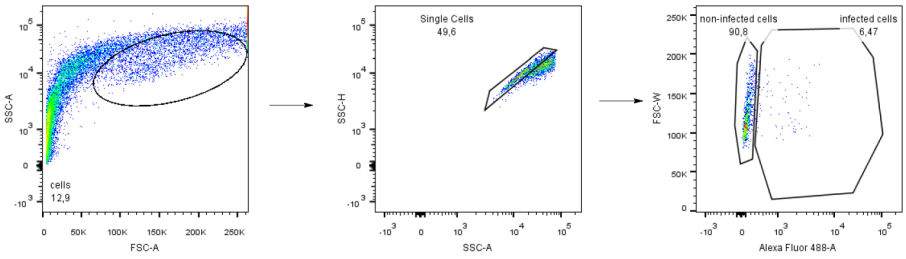

b.

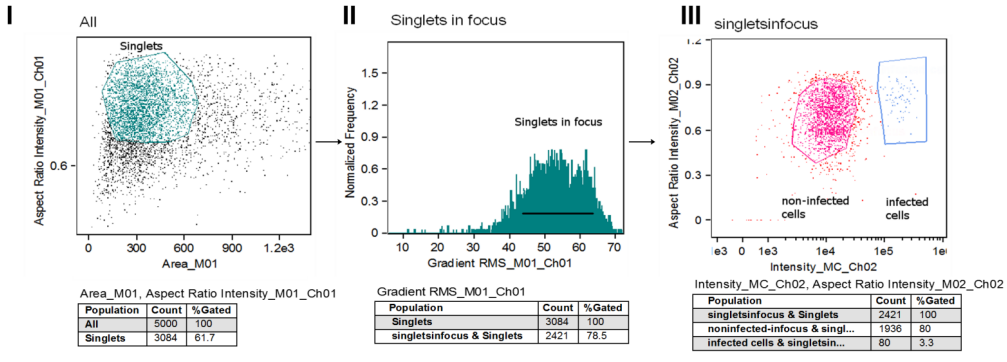

Area_M01, Aspect Ratio Intensity_M01_Ch01

Population	Count	%Gated
All	5000	100
Singlets	3084	61.7

Gradient RMS_M01_Ch01

Population	Count	%Gated
Singlets	3084	100
singletsinfocus & Singlets	2421	78.5

Intensity_MC_Ch02, Aspect Ratio Intensity_M02_Ch02

Population	Count	%Gated
singletsinfocus & Singlets	2421	100
noninfected-infocus & singl...	1936	80
infected cells & singletsin...	80	3.3

Intensity_MC_Ch04

Population	Count	%Total	%Gated
noninfected-infocus & sing...	1936	38.7	100

Intensity_MC_Ch04

Population	Count	%Total	%Gated
infected cells & singletsi...	80	1.6	100

c.1.

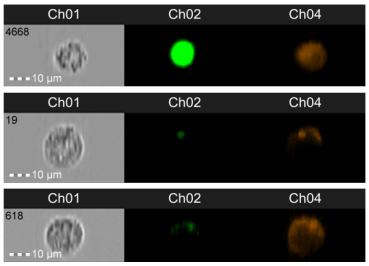

2b- inf

2b - noninf

2b - naive

c.2

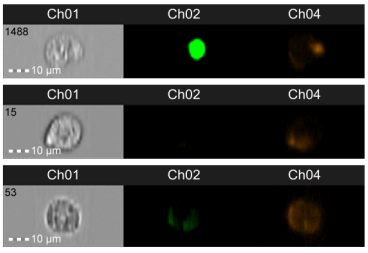

9 - inf

9 - noninf

9 - naive

Figure S6: a.1/2. Gating strategy during the analysis of metabolic incorporation of **2b** in HepG2 cell membrane glycans by flow cytometry, selection of live cells, single cells and infected vs. non-infected cells. **b.** Gating strategy during the analysis of metabolic incorporation of **2b** in HepG2 cell membrane glycans by imaging flow cytometry, selection of single cells (I), single cells in focus (II), separation of infected and non-infected cells based on the intensity of GFP (Ch02, III), Fluorescence intensity resulting of the incorporation of **2b** in non-infected (IV) and infected cells (V). **c.1.** representative pictures acquired in Amnis ImageStreamX MarkII, HepG2 cells after metabolic incorporation of **2b**, infected, non_infected and naïve. **c.2.** representative pictures acquired in Amnis ImageStreamX MarkII, HepG2 cells after metabolic incorporation of contol **9**, infected, non-infected and naïve.

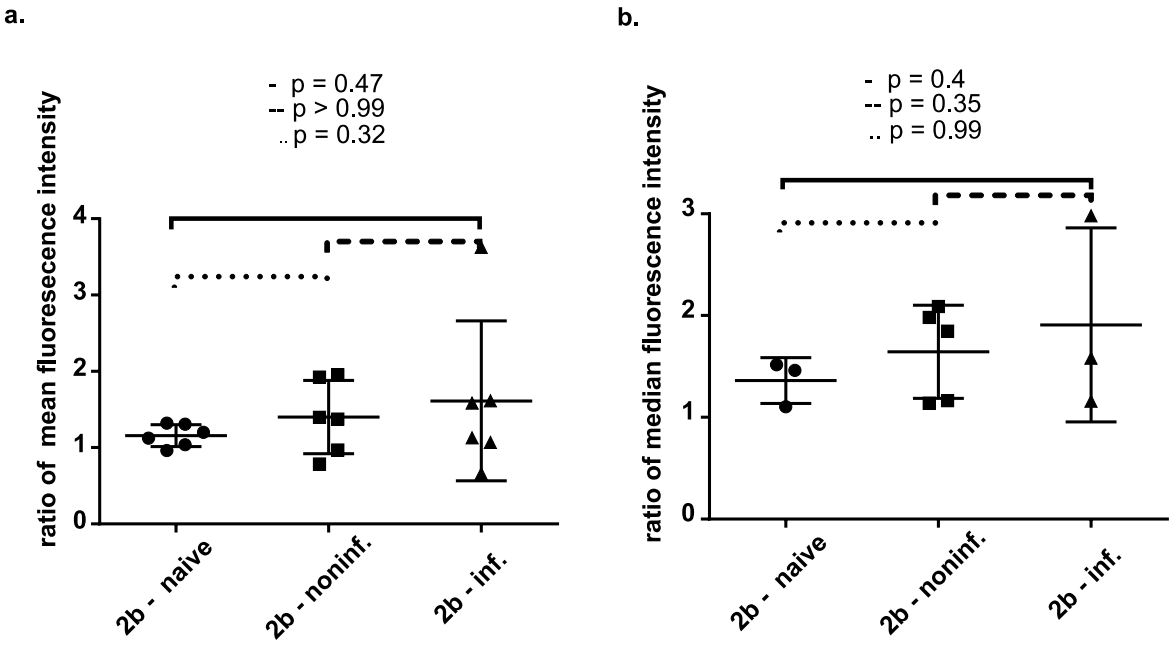

Figure S7: a. Quantification of fluorescence intensity resulting from incorporated galactose derivative **2b** by confocal point-scanning microscopy, Data representative from one experiment out of three, each data point represents the mean fluorescence intensity of all single cells within one picture, two-tailed Mann-Whitney test. **b.** Quantification of fluorescence intensity resulting from incorporated galactose derivative **2b** by flow cytometry, Combined data from three independent experiments, each data point represents the median intensity of 2000-3000 gated single cells, two-tailed Mann-Whitney test.

a.

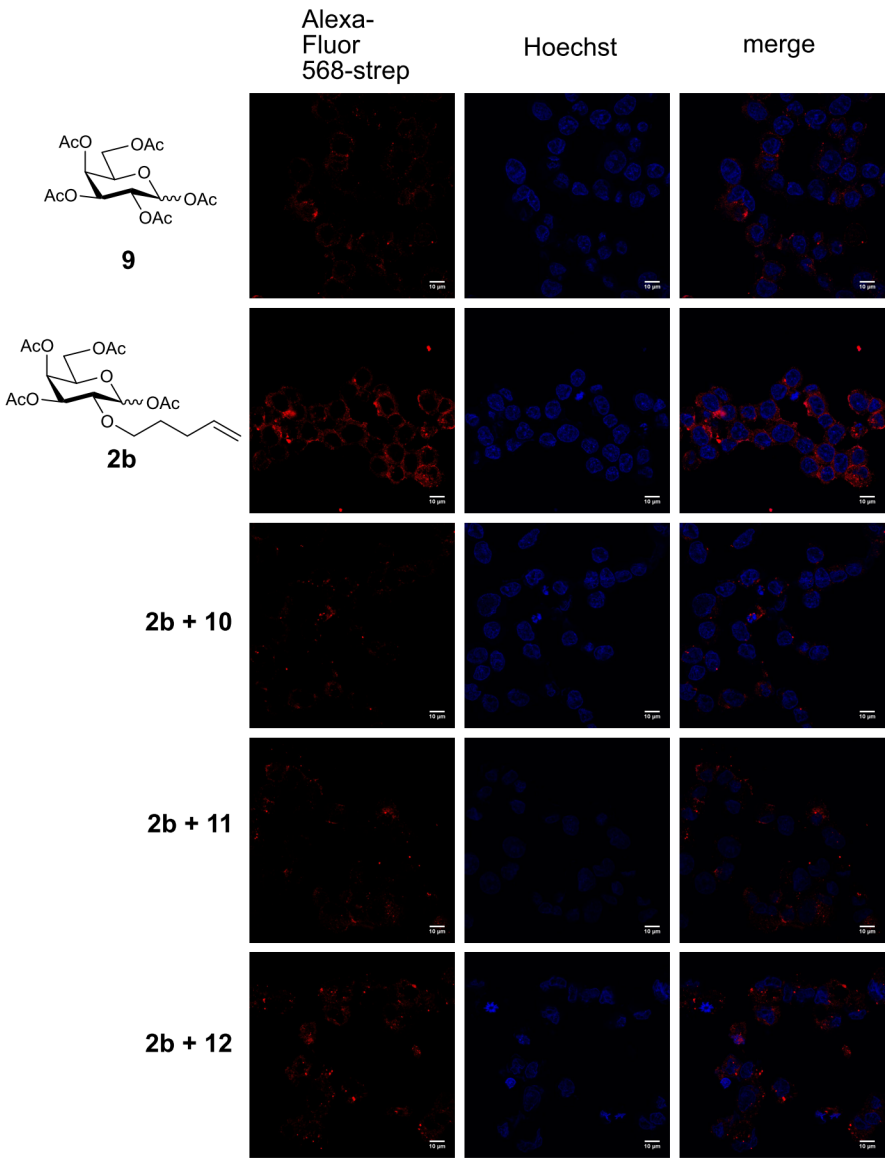
Alexa-
Fluor
568-strep
Hoechst
merge
AcO
OAc
O
AcO
OAc
OAc
9
AcO
OAc
O
AcO
OAc
O
2b
2b + 10
2b + 11
2b + 12

b.

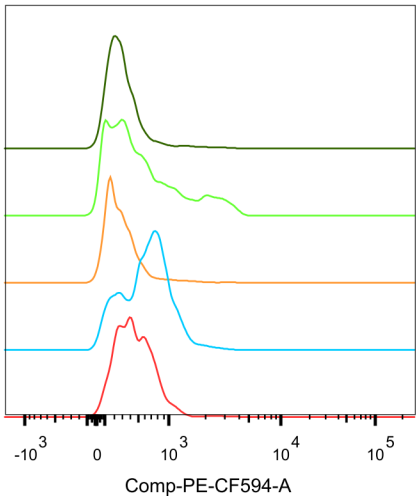
-10 3
0
10 3
10 4
10 5
Comp-PE-CF594-A

Figure S8: a. Metabolic incorporation of **2b** into HepG2 cell membrane glycans, without and in presence of inhibitors **10**-**12**. Pentaacetyl galactose **9** was used as negative control. **b.** Half-offset histograms of fluorescence intensity in channel PE-CF594-A, normalized mode, after metabolic incorporation of derivative **2b** in HepG2 cells, without inhibitor (blue), with increasing concentrations of WZB117 **10**, 10 μM (orange), 20 μM (green), 30 μM (dark green). Pentaacetyl galactose **9** was used as negative control.

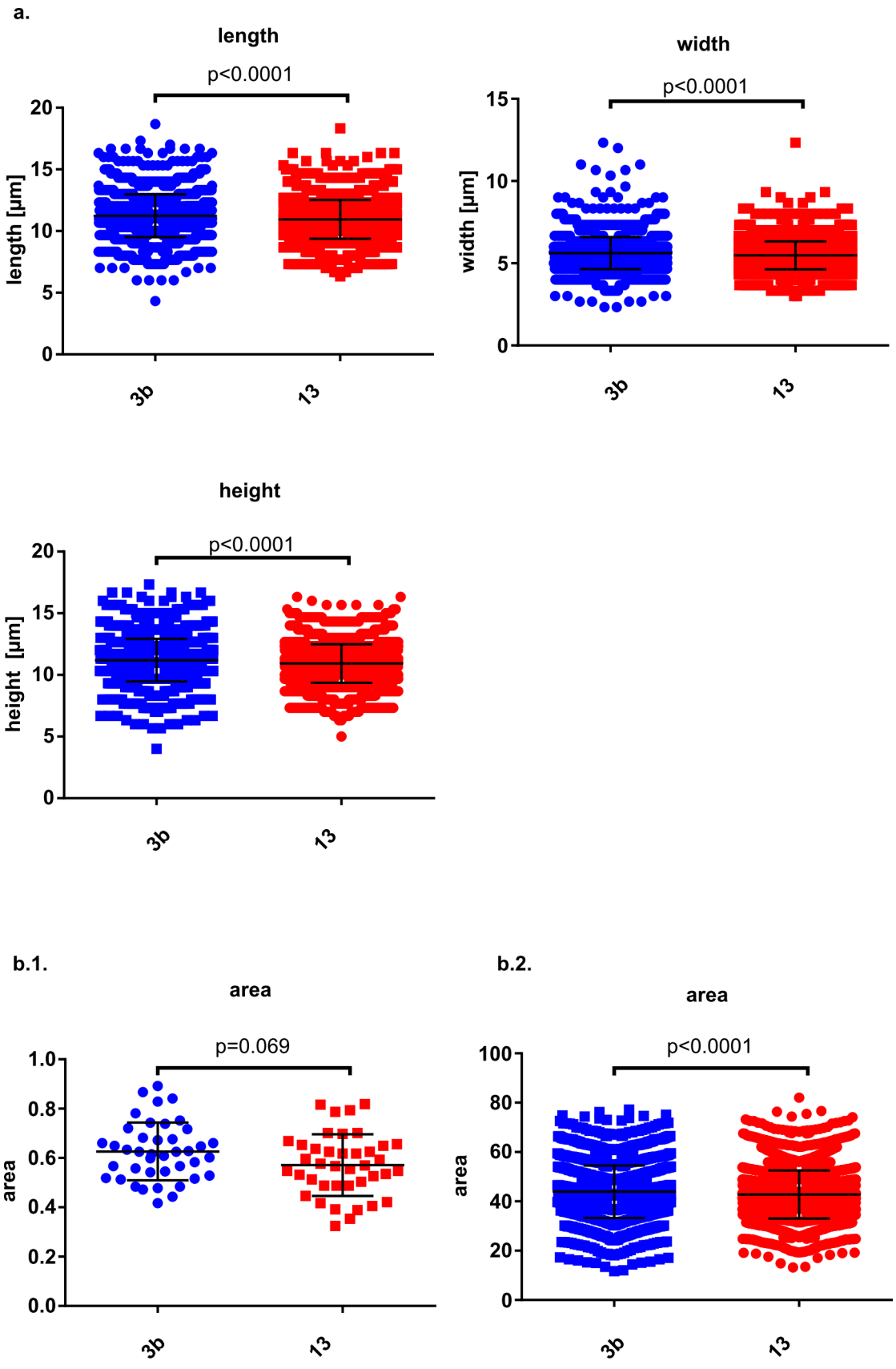
a.
length
p<0.0001
length [µm]
20
15
10
5
0
3b
13
width
p<0.0001
width [µm]
15
10
5
0
3b
13
height
p<0.0001
height [µm]
20
15
10
5
0
3b
13
b.1.
area
p=0.069
area
1.0
0.8
0.6
0.4
0.2
0.0
3b
13
b.2.
area
p<0.0001
area
100
80
60
40
20
0
3b
13

Figure S9: a. Shape parameters of *Plasmodium berghei* parasites after feeding with **3b** or control **13**, acquisition in Amnis ImageStreamX MarkII, two-tailed Mann-Whitney. **b.1.** Determination of the parasite size/area of representative pictures acquired with Amnis ImageStreamX MarkII, measurements were performed using ImageJ software package, n = 50, two-tailed Mann-Whitney. **b.2.** Determination of the parasite size/area of all acquired pictures with Amnis ImageStreamX MarkII, n=2000-3000, two-tailed Mann-Whitney.

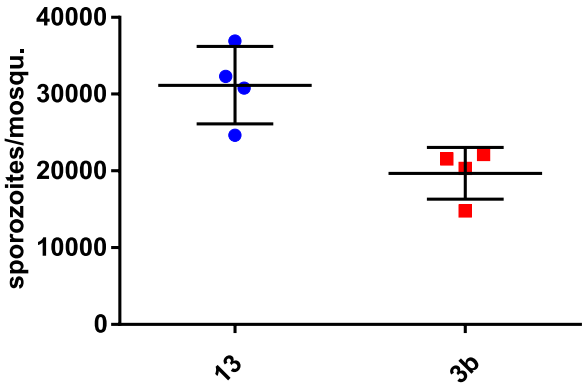

Figure S 10: Sporozoite number per mosquito, for mosquitoes receiving galactose derivative **3b** or control **13**.

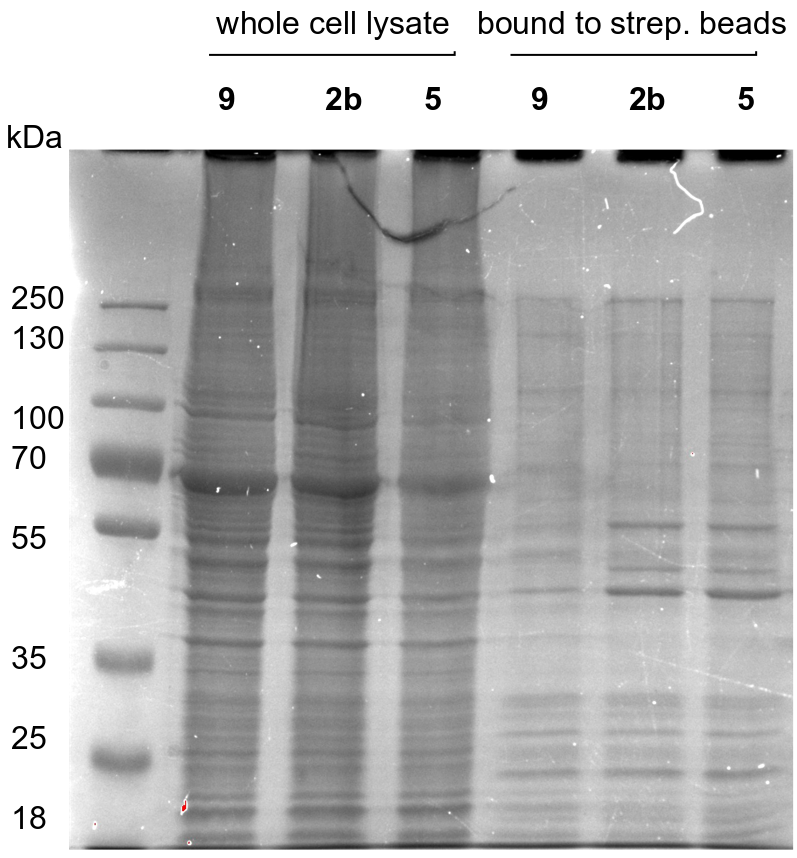

Figure S11: Coomassie blue staining of whole protein cell lysate and protein samples bound to streptavidin magnetic beads from HepG2 cells, cells were grown for 72h with 100 µM of **9**, **2b** or **5**.

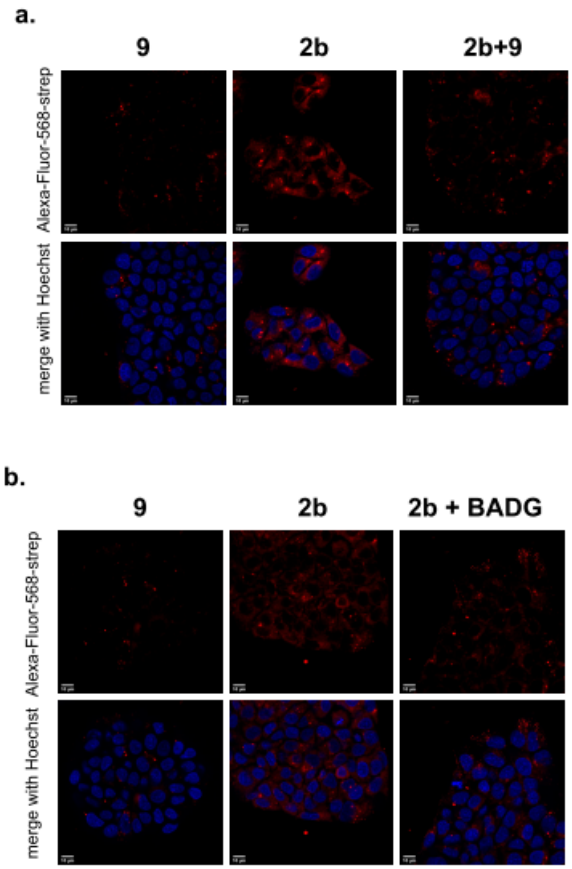

Figure S12: HepG2 cells grown with 500 µM **9** or **2b**, for a competition experiment both **9** and **2b** were added simultaneously. **b.** HepG2 cells were grown with 100 µM of **9** or **2b**, Benzyl-2-acetamido-2-deoxy-galactopyranse (BADG) was added with 100 µM after 24h to a culture with **2b** and the cells were analysed after a total culture time of 72h. IEDDA reaction was performed with 6-methyl-tetrazine-peg4-biotin, followed by staining with Alexa-Fluor-568-streptavidin (red) and Hoechst (blue).

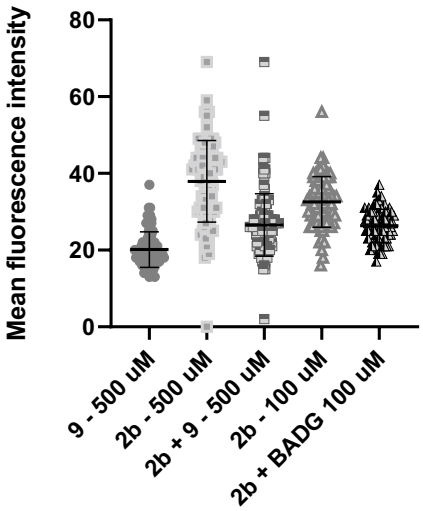

Figure S13: Mean Fluorescence intensity of single cells, after incorporation of control **9** or **2b**, in concentrations of 500 or 100 µM, competition experiment with **9** and **2b**, in the presence of inhibitor Benzyl-2-acetamido-2-deoxy-galactopyranse (BADG). 7-8 pictures from different positions in the well were analyzed.

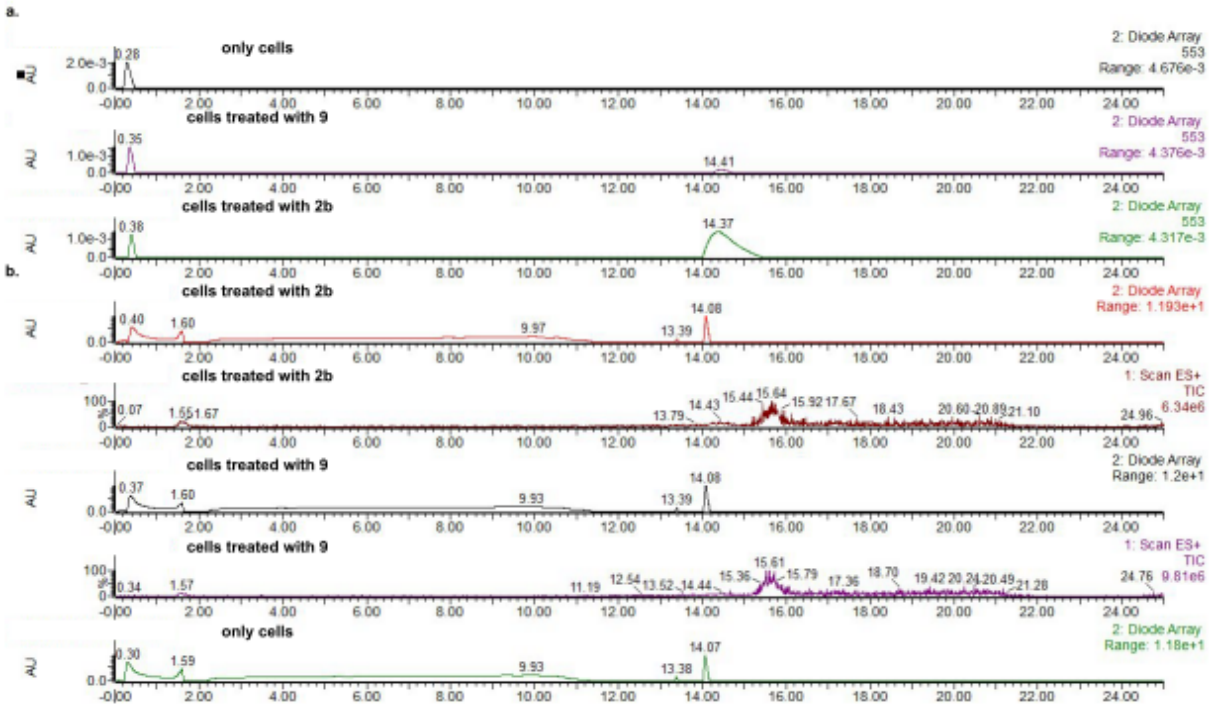

Figure S14: Analysis of cell surface glycans released by tryptic digestion and labelled with 6-methyl-tetrazine-sulfo-Cy3, **a.** Analysis at 553 nm, representing specific tetrazine absorbance **b.** UV (200-650 nm) and ES+ trace of all samples.

2. General Procedures

The used reagents were purchased from Alfa Aesar, Carbosynth Limited, Fisher Scientific and Sigma Aldrich and were used without further purification. Purification of the compounds was performed by chromatography using Silica Gel 60 (mesh 230-400) from Material Harvest. Thin layer chromatography (TLC) was carried out on silica gel coated aluminium plates (60 F_{254}, Merck) and the reactions were visualized with 5% sulfuric acid in ethanol and UV light (λ =254 nm). Proton (^{1}H NMR), carbon (^{13}C NMR) nuclear magnetic resonance spectra were recorded on a Bruker 500 MHz DCM Cryoprobe or 400 MHz DPX-400 Dual spectrometer. All spectra were fully assigned using COESY, HSQC and HMBC, the chemical shifts were quoted on the δ scale in ppm and the solvent peak ($CDCl_3$: ^{1}H = 7.26 ppm, ^{13}C = 77.16 ppm, D_2O: ^{1}H = 4.79 ppm) was used as internal standard. Coupling constants *J* were reported in Hz, using the following splitting abbreviations: s = singlet, d = duplet, t = triplet, dd = duplet from duplet, m = multiplet. High resolution mass spectrometry (HRMS) were received from a Thermo Finnigan Orbitrap Classic using positive ion electronstpray ionization (ESI) for essential compounds.

2.1. Chemical Synthesis

2.1.1. Synthesis of 2-*O*-allyl-1,3,4,6-tetra-*O*-acetly-galactopyranose (2a)

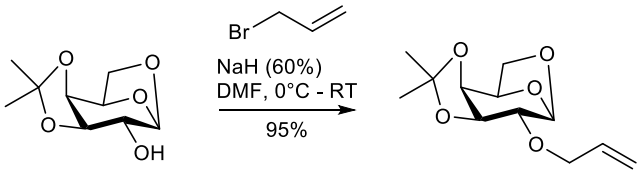

1,6-Anhydro-3,4-isopropylgalactopranose (300 mg, 1.48 mmol) was dissolved in 6 mL anhydrous DMF and cooled to 0 °C. NaH (60% suspension in mineral oil, 149 mg, 4.45 mmol) was added and the reaction was stirred for 30 min. Allylbromid (0.387 mL, 4.45 mmol) was added slowly and the reaction was stirred over night from 0 °C – RT. Water was added carefully. The reaction mixture was extracted with CH_2Cl_2, the organic layer was washed three times with 5 mL of

saturated sodium chloride solution, dried with $MgSO_4$, filtrated through a cotton patch and concentrated. The product 1,6-anhydro-2-allyl-3,4-isopropylgalactose was obtained after column chromatography (petrol/EtOAc 3:1) with a yield of 95% (339.8 mg, 1.4 mmol).

^{1}H-NMR (300 MHz, $CDCl_3$): δ = 5.88 (ddt, J = 17.2 Hz, J =10.4 Hz, J = 5.6 Hz, 1H, C***H***=CH_2), 5.38 (s, 1H, ***H***1), 5.28 (dq, J = 17.2, J = 1.5 Hz, 1H, CH=C***H₂***), 5.19 (ddd, J = 10.4 Hz, J = 2.7 Hz, J = 1.2 Hz, 1H, CH=C***H₂***), 4.46 (t, J = 5.6 Hz, 1H, ***H***3), 4.40 (t, J = 6.4 Hz, 1H, ***H***5), 4.14 (dd, J = 5.9, J = 4.9 Hz, 1H, ***H***4), 4.12 – 4.06 (m, 2H, ***H***6), 4.06 – 4.00 (m, 1H, C***H₂***-CH), 3.53 (dt, J = 10.2, J = 4.2 Hz, 1H, C***H₂***-CH), 3.48 (s, 1H, ***H***2), 1.49 (s, 3H, C***H₃***), 1.32 (s, 3H, C***H₃***) ppm.

^{13}C-NMR (75 MHz, $CDCl_3$): δ = 133.81 (***C***H=CH_2), 117.79 (CH=***C***H_2), 108.36 (***C***$(CH_3)_2$), 99.60 (***C***1), 76.56 (***C***2), 74.05 (***C***4), 71.92 (***C***3), 71.06 (***C***6), 69.21 (***C***5), 62.89 (O***C***H_2-CH=CH_2), 25.66 (***C***H_3), 24.17 (***C***H_3) ppm.

HRMS-ESI+ (m/z): calculated [M + H^+] = 243.1227, found [M + H^+] = 243.1240

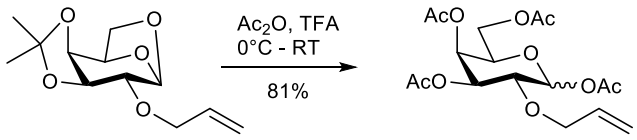

The obtained material (339.8 mg, 1.4 mmol) was dissolved in Ac_2O (7.5 mL/ mmol) and cooled to 0 °C. Trifluoracetic acid (TFA, 1.26 mL/mmol) was added dropwise and the reaction was stirred overnight from 0 °C – RT. The reaction was diluted with EtOAc (10 mL) and washed with saturated solution of sodium bicarbonate (3 x 10 mL) and saturated sodium chloride solution (2 x 10 mL). The organic layer was dried with $MgSO_4$, filtrated through a cotton patch and concentrated. The crude mixture was purified by column chromatography (petrol/ EtOAc 3:1 -> 1:1) and the product 2-allyl-1,3,4,6-*O*-acetyl-galactopyranose was obtained with a yield of 81% (444.3 mg, 1.14 mmol).

^{1}H-NMR (400 MHz, $CDCl_3$): δ = 6.39 (d, J = 3.6 Hz, 1H, ***H***1α), 5.82 (ddd, J = 22.8 Hz, J = 10.8 Hz, J = 5.6 Hz, 1H, C***H***=CH_2), 5.61 (d, J = 8.2 Hz, 1H, ***H***1β), 5.46 (d, J = 2.2 Hz, 1H, ***H***4α), 5.39 (d, J = 2.7 Hz, 1H, ***H***4β), 5.26 (dd, J = 13.5 Hz, J = 2.4 Hz, 1H, CH=C***H***$_2$), 5.22 (dd, J = 6.6 Hz, J = 3.3 Hz, 1H, ***H***3α), 5.19 (dd, J = 10.5 Hz, J = 1.2 Hz, 1H, CH=C***H***$_2$), 4.99 (dd,

J = 10.1 Hz, J = 3.4 Hz, 1H, ***H***3β), 4.28 (t, J = 6.7 Hz, 1H, ***H***5), 4.10 – 4.04 (m, 4H, ***H***6a/b, OC$\boldsymbol{H}_2$), 3.87 (dd, J = 10.6 Hz, J = 3.6 Hz, 1H, ***H***2α), 3.68 (dd, J = 10.1 Hz, J = 8.2 Hz, 1H, ***H***2β), 2.15, 2.14, 2.03, 2.02 (4 × s, 4 × 3H, C$\boldsymbol{H}_3$CO) ppm.

^{13}C-NMR (100 MHz, $CDCl_3$): δ = 170.6, 170.3, 170.2, 169.4 (4 × $CH_3\boldsymbol{C}O$), 134.2 (***C***H=CH_2), 117.9 (CH=***C***H_2), 90.2 (***C***1), 72.3 (***C***2), 72.2 (O***C***H_2), 69.5 (***C***3), 68.7 (***C***5), 67.9 (***C***4), 61.5 (***C***6), 21.1, 20.9, 20.8, 20.7 (4 × ***C***H_3CO) ppm.

HRMS-ESI+ (m/z): calculated [M + H^+] = 389.1442, found [M+ H^+] = 389.1440

2.1.2. Synthesis of 2-*O*-allyl-galactopyranose (3a)

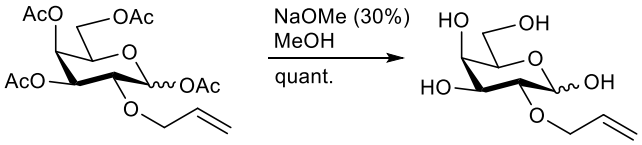

The fully acetylated sugar 2-allyl-1,3,4,6-tetra-*O*-acetyl-galactopyranose (100 mg, 0.257 mmol) was dissolved in 2 mL MeOH and 30% NaOMe solution (0.142 mL) was added. The reaction was stirred at RT until TLC showed complete consumption of the starting material. The mixture was neutralized with Dowex 50W (H^+ from), filtrated and concentrated. The final, unprotected monosaccharide was purified by chromatography (EtOAc/MeOH 3:1) and obtained in quantitative yield as mix of both anomers.

^{1}H-NMR (400 MHz, D_2O): δ = 6.06 – 5.92 (m, 2H, C***H***=CH_2, C***H'***=CH_2), 5.44 (d, J = 3.7 Hz, 1H, ***H***1α), 5.41 – 5.25 (m, 4H, CH=C$\boldsymbol{H}_2$, CH=C$\boldsymbol{H'}_2$) , 4.64 (d, J = 7.9 Hz, 1H, ***H***1β), 4.34 (ddd, J = 39.2 Hz, J = 12.1 Hz, J = 6.2 Hz, 2H, ***H***6'), 4.23 – 4.15 (m, 2H, OC$\boldsymbol{H}_2$), 4.07 (dd, J = 11.8 Hz, J = 5.5 Hz, 1H, ***H***3'), 4.00 (d, J = 2.9 Hz, 1H, ***H***3'), 3.97 – 3.88 (m, 1H, ***H***4), 3.79 – 3.71 (m, 2H, ***H***6), 3.71 – 3.64 (m, 2H, ***H***3, ***H***2'), 3.39 (dd, J = 9.9 Hz, J = 8.4 Hz, 1H, ***H***2) ppm.

^{13}C NMR (101 MHz, D_2O): δ = 134.1 (***C***H=CH_2), 118.5 (CH=***C***H_2), 96.4 (***C***1), 90.3 (***C***1'), 79.9 (***C***2), 75.6 (***C***2'), 73.9 (***C***6'), 72.4 (***C***3), 71.5 (O***C***H_2), 70.2 (***C***3'), 69.3 (***C***5), 68.8 (***C***4), 61.1(***C***6, ***C***6'), 60.9 (***C***6, ***C***6') ppm.

Signals assigned with ‘ represent the alpha-conformer.

2.1.3. Synthesis of 2-*O*-pentenyl-1,3,4,6-tetra-*O*-acetyl-galactopyranose (2b)

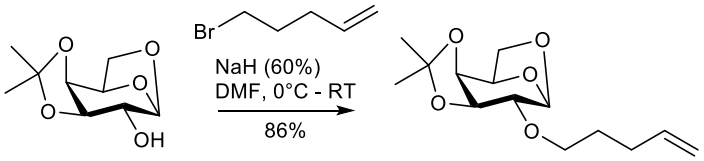

1,6-Anhydro-3,4-isopropylgalactopranose (300 mg, 1.48 mmol) was dissolved in 6 mL anhydrous DMF and cooled to 0 °C. NaH (60% suspension in mineral oil, 149 mg, 4.45 mmol) was added and the reaction was stirred for 30 min. 5-Bromo-1-pentene (0.387 mL, 4.45 mmol) was added slowly and the reaction was stirred over night from 0 °C – RT. Water was added carefully. The reaction mixture was extracted with CH_2Cl_2, the organic layer was washed three times with 5 mL of saturated sodium chloride solution, dried with $MgSO_4$, filtrated through a cotton patch and concentrated. The product 1,6-anhydro-2-pentenyl-3,4-isopropylgalactose was obtained after column chromatography (petrol/EtOAc 3:1) with a yield of 86% (343.8 mg, 1.27 mmol).

^{1}H-NMR (500 MHz, $CDCl_3$): δ = 5.80 (ddt, $J_{CH/CH2=CH}$ = 16.9 Hz, $J_{CH/CH2=CH}$ = 10.2 Hz, $J_{CH/CH2}$ = 6.7 Hz, 1H, C***H***=CH_2), 5.41 (d, $J_{H1/H2}$ = 1.3 Hz, 1H, ***H***1), 5.03 (dq, $J_{CH2=CH/CH}$ = 17.1 Hz, $J_{CH2=CH/CH2=CH}$ = 1.7 Hz, 1H, CH=C***H***$_2$), 4.97 (m,1H, CH=C***H***$_2$), 4.50 (t, $J_{H6/H6,5}$ = 5.7 Hz, 1H, ***H***6), 4.46 – 4.41 (m, 1H, ***H***4), 4.16 (dt, $J_{H3/H4}$ = 7.2 Hz, $J_{H3/H1}$ = 1.1 Hz, 1H, ***H***3), 4.08 (d, $J_{H6/H5}$ = 7.5 Hz, 1H, ***H***6), 3.64 – 3.60 (m, 1H, ***H***5), 3.60 – 3.55 (m, 2H, O-C***H***$_2$), 3.43 (d, $J_{HH2/H1}$ = 0.9 Hz, 1H, ***H***2), 2.13 (m, 2H, C***H***$_2$-CH=CH_2), 1.70 (m, 2H, C***H***$_2$-CH_2-O), 1.53 (s, 3H, C***H***$_3$), 1.36 (s, 3H, C***H***$_3$) ppm.

^{13}C NMR (120 MHz, $CDCl_3$): δ = 138.1 (***C***H=CH_2), 115.2 (CH=***C***H_2), 99.9 (***C***1), 78.3 (***C***2), 74.3 (***C***3), 72.2 (***C***6), 69.5 (***C***6), 63.2 (***C***H_2O), 31.1, 30.3 (***C***H_2-CH=CH_2), 28.9 (***C***H_2-CH_2O), 25.9 (***C***H_3), 24.5 (***C***H_3) ppm.

HRMS-ESI+ (m/z): calculated [M + H^+] = 271.1540, found [M + H^+] = 271.1546

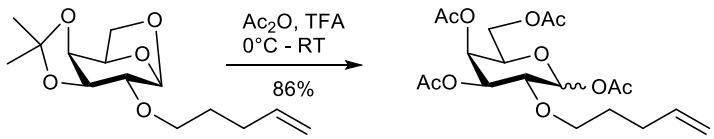

The obtained material (343.8 mg, 1.27 mmol) was dissolved in Ac_2O (7.5 mL/ mmol) and cooled to 0 °C. Trifluoracetic acid (TFA, 1.26 mL/mmol) was added dropwise and the reaction was stirred overnight from 0 °C – RT. The reaction was diluted with EtOAc (10 mL) and washed with saturated solution of sodium bicarbonate (3 x 10 mL) and saturated sodium chloride solution (2 x 10 mL). The organic layer was dried with $MgSO_4$, filtrated through a cotton patch and concentrated. The crude mixture was purified by column chromatography (petrol/ EtOAc 3:1 -> 1:1) and the product 2-pentenyl-1,3,4,6-*O*-acetyl-galactopyranose was obtained with a yield of 86% (455.6 mg, 1.09 mmol).

^{1}H-NMR (400 MHz, $CDCl_3$): δ = 6.41 (d, J = 3.6 Hz, 1H, ***H***1α), 5.77 (ddt, J = 16.9 Hz, J = 10.1 Hz, J = 6.7 Hz, 1H, C***H***=CH_2), 5.59 (d, J = 8.1 Hz, 1H, ***H***1β), 5.46 (d, J = 2.4 Hz, 1H, ***H***4α), 5.38 (d, J = 3.1 Hz, 1H, ***H***4β), 5.20 (dd, J = 10.5 Hz, J = 3.2 Hz, 1H, ***H***3α), 5.04 – 4.92 (m, 3H, ***H***3β, CH=C***H***$_2$), 4.28 (t, J = 6.6 Hz, 1H, ***H***5α), 4.07 (dd, J = 6.7 Hz, J = 2.0 Hz, 2H, ***H***6a/b), 3.78 (dd, J = 10.5 Hz, J = 3.6 Hz, 1H, ***H***2α), 3.63 (ddd, J = 15.2 Hz, J = 11.1 Hz, J = 4.6 Hz, 2H, ***H***2β, OC***H***$_2$), 3.48 (dt, J = 9.1 Hz, J = 6.5 Hz, 1H, OC***H***$_2$), 2.15 (2 × s, 6H, C***H***$_3$), 2.06 (d, J = 5.3 Hz, 2H, OCH_2CH_2C***H***$_2$), 2.03, 2.02 (2 × s, 6H, C***H***$_3$), 1.63 – 1.55 (m, 2H, OCH_2C***H***$_2$) ppm.

^{13}C-NMR (100 MHz, $CDCl_3$): δ = 170.7, 170.4, 170.3, 169.4 (4 × CH_3***C***O), 138.1 (***C***H=CH_2), 115.1 (CH=***C***H_2), 94.1 (***C***1β), 90.1 (***C***1) 73.2 (***C***2), 70.9 (O***C***H_2), 69.4 (***C***3), 68.7 (***C***5), 67.9 (***C***3), 61.5 (***C***6), 29.9 (OCH_2CH_2***C***H_2), 29.1 (OCH_2***C***H_2), 21.1, 20.9, 20.8, 20.7 (4 × ***C***H_3CO) ppm.

HRMS-ESI+ (m/z): calculated [M + Na^+] = 439.1575, found [M + Na^+] = 439.1571

2.1.4. Synthesis of 2-*O*-pentenyl-galactopyranose (3b)

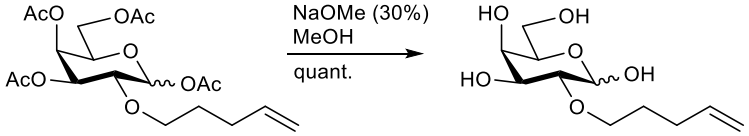

2-*O*-pentenyl-1,3,4,6-*O*-acetyl-galactopyranose (100 mg, 0.24 mmol) was dissovled in 2 mL MeOH and 30% NaOMe solution (0.136 mL) was added. The reaction was stirred at RT until TLC showed complete consumption of the starting material. The mixture was neutralized with Dowex 50W (H^+ form), filtrated and concentrated. The final, unprotected monosaccharide was purified by chromatography (EtOAc/MeOH 3:1) and was obtained in quantitative yield.

^{1}H NMR (400 MHz, D_2O) δ = 6.00 – 5.85 (m, 2H, C***H***=CH_2, C***H'***=CH_2), 5.44 (d, J = 3.5 Hz, 1H, ***H***1α), 5.10 (d, J = 17.3 Hz, 2H, CH=C***H***$_2$, CH=C***H'***$_2$), 5.03 (d, J = 10.2 Hz, 2H, CH=C***H***$_2$, CH=C***H'***$_2$), 4.62 (d, J = 7.9 Hz, 1H, ***H***1β), 4.08 (dd, J = 11.5 Hz, J = 5.3 Hz, 1H, ***H***5'), 3.96 (dd, J = 25.6 Hz, J = 2.7 Hz, 2H, ***H***4, ***H***5), 3.92 – 3.84 (m, 2H, ***H***3α, OC***H***$_2$), 3.82 – 3.63 (m, 10H, OC***H***$_2$, OC***H'***$_2$, ***H***3', ***H***4', ***H***6a,b, ***H***6'a,b), 3.60 (dd, J = 10.3 Hz, J = 3.9 Hz, 1H, ***H***2'), 3.35 – 3.27 (m, 1H, ***H***2), 2.15 (q, J = 7.0 Hz, 4H, C***H***$_2$CH=CH_2, C***H'***$_2$CH=CH_2), 1.76 – 1.67 (m, 4H, OCH_2C***H***$_2$, OCH_2C***H'***$_2$) ppm.

^{13}C NMR (101 MHz, D_2O) δ = 139.0, 138.9 (***C***H=CH_2, ***C***'H=CH_2), 114.7 (CH=***C***H_2), 96.3 (***C***1β), 90.2 (***C***1α), 80.3 (***C***2), 76.3 (***C***2'), 75.0 (***C***3), 72.6 (O***C***H_2), 72.4 (***C***3/***C***4'), 70.2 (***C***5'), 70.0 (O***C***H_2), 69.3 (***C***5), 68.8 (***C***4), 68.4 (***C***3'), 61.14, 60.89 (***C***6, ***C***6') 29.4 (***C***H_2CH=CH_2), 28.2 (OCH_2***C***H_2) ppm.

2.1.5. Synthesis of 6-*O*-pentenyl-1,2,3,4-tetra-*O*-acetyl-galactopyranose (5)

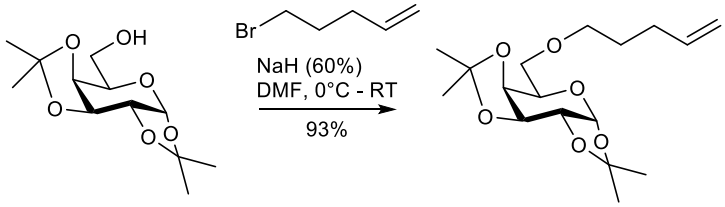

The monosaccharide 1,2,3,4-diisopropyl-galactopyranose (300 mg, 1.15 mmol) was dissovled in 5 mL anhydrous DMF and cooled to 0 °C. NaH (60% suspension in mineral oil, 116 mg, 3.46 mmol) was added and the mixture was stirred for 30 min. 5-Bromo-1-pentente (0.409 mL, 3.46 mmol) was added slowly to the reaction and the mixture was stirred overnight from 0 °C to

RT. 2 mL of water were added carefully to the reaction and the mixture was extracted with CH_2Cl_2 (3 x 5 mL). The organic layer was washed with saturated sodium chloride solution (3 x 5 mL), dried with $MgSO_4$, filtrated through a cotton patch and concentrated. The crude mixture was purified by chromatography (petrol/EtOAc 3:1 -> 1:1) and the product 6-*O*-pentenyl-1,2,3,4—diisopropyl-galactopyranose was obtained with a yield of 93% (350 mg, 1.07 mmol)

^{1}H-NMR (400 MHz, $CDCl_3$): δ = 5.87 – 5.74 (m, 1H, C***H***=CH_2), 5.53 (d, *J* = 5.0 Hz, 1H, ***H***1), 5.05-4.97 (m, 1H, CH=C***H***$_2$), 4.97-4.91 (m, 1H, CH=C***H***$_2$), 4.59 (dd, *J* = 7.9 Hz, *J* = 2.3 Hz, 1H, ***H***3), 4.29 (dd, *J* = 5.0 Hz, *J* = 2.4 Hz, 1H, ***H***2), 4.25 (dd, *J* = 7.9 Hz, *J* = 1.8 Hz, 1H, ***H***4), 3.95 (td, *J* = 6.3 Hz, *J* = 1.8 Hz, 1H, ***H***5), 3.66 – 3.53 (m, 2H, ***H***6), 3.53 – 3.44 (m, 2H, OC***H***$_2$$CH_2$), 2.15-2.06 (m, 2H, C***H***$_2$CH=CH_2), 1.67 (dt, *J* = 13.7 Hz, *J* = 6.7 Hz, 2H, OCH_2C***H***$_2$), 1.53, 1.44,1.33, 1.32 (4 × s, 4 × 3H C***H***$_3$) ppm.

^{13}C-NMR (100 MHz, $CDCl_3$): δ = 138.5 (***C***H=CH_2), 114.8 (CH=***C***H_2), 109.3, 108.6 (2 × ***C***$(CH_3)_2$), 96.5 (***C***1), 71.3 (***C***4), 70.9, 70.8 (***C***2, ***C***3, O***C***H_2CH_2), 69.4 (***C***6), 66.8 (***C***5), 30.4 (***C***H_2CH=CH_2), 28.9 (OCH_2***C***H_2), 26.2, 26.1, 25.1, 24.6 (4 × ***C***H_3) ppm.

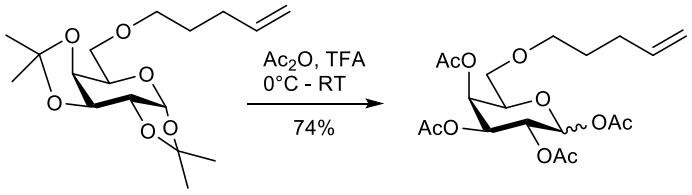

The sugar 6-*O*-pentenyl-1,2,3,4-diisopropyl-galactopyranose (350 mg, 1.07 mmol) was dissolved in Ac_2O (8.33 mL, 7.5 mL/mmol) and cooled to 0 °C. TFA (1.39 mL, 1.26 mL/mmol) was added dropwise and the reaction was stirred from 0 °C-RT overnight. The reaction was diluted with EtOAc and the organic layer was washed with saturated solution of sodium bicarbonate (3 x 5 mL), saturated sodium chloride solution (2 x 5 mL), dried with $MgSO_4$, filtrated and concentrated. The crude mixture was purified by chromatography (petrol/EtOAc 4:1 -> 2:1) and the product was obtained with a yield of 74% (0.79 mmol, 329 mg).

^{1}H-NMR (500 MHz, $CDCl_3$): δ = 6.35 (d, *J* = 2.7 Hz, 1H, ***H***1), 6.08 (d, *J* = 1.5 Hz, 1H, ***H***1'), 5.82-5.70 (m, 1H, C***H***=CH_2), 5.53 (s, 1H, ***H***3), 5.32 (t, *J* = 2.8 Hz, 1H, ***H***2), 4.99 (dd, *J* = 17.1 Hz,

J = 1.4 Hz, 1H, CH=C***H***$_2$), 4.93 (d, *J* = 10.2 Hz, 1H, CH=C***H***$_2$), 4.24 (dd, *J* = 13.3 Hz, *J* = 6.8 Hz, 1H, ***H***4), 3.49 – 3.29 (m, 5H, ***H***5, ***H***6a/b, OC***H***$_2$CH$_2$), 2.13 (s, 6H, 2 × C***H***$_3$CO), 2.07 (dd, *J* = 5.2 Hz, *J* = 2.6 Hz, 2H, C***H***$_2$CH=CH$_2$), 2.00, 1.98 (2 × s, 6H, 2 × C***H***$_3$CO), 1.63 – 1.56 (m, 2H CH$_2$C***H***$_2$CH$_2$) ppm.

^{13}C-NMR (126 MHz, $CDCl_3$): δ = 170.3, 170.2, 170.1, 169.2 (4 × CH$_3$***C***O), 138.2 (***C***H=CH$_2$), 114.9 (CH=***C***H$_2$), 89.9 (***C***1), 71.2 (O***C***H$_2$CH$_2$), 70.1 (***C***4), 68.4 (***C***6), 68.1 (***C***3), 67.7, 66.8 (***C***2), 30.1 (***C***H$_2$CH=CH$_2$), 28.7 (CH$_2$***C***H$_2$CH$_2$), 20.8, 20.7, 20.6, 20.5 (4 × ***C***H$_3$CO) ppm.

HRMS-ESI+ (m/z): calculated [M + Na$^+$] = 439.1575, found [M + Na$^+$] = 439.1571

2.1.6. Synthesis of 6-*O*-pentenyl-galactopyranose (6)

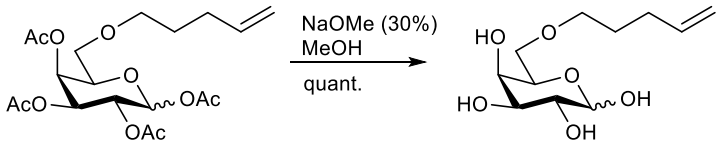

6-*O*-pentenyl-1,2,3,4-tetra-*O*-acetyl-galactopyranose (100 mg, 0.24 mmol) was dissovled in 2 mL MeOH and 30% NaOMe solution (0.136 mL) was added. The reaction was stirred at RT until TLC showed complete consumption of the starting material. The mixture was neutralized with Dowex 50W (H^+ form), filtrated and concentrated. The final, deprotected monosaccharide 6-*O*-pentenyl-galactopyranose was obtained after chromatography (EtOAc/MeOH 3:1) in quantitative yield.

^{1}H-NMR (400 MHz, D_2O): δ = 5.92 (ddt, *J* = 16.9 Hz, *J* = 10.4 Hz, *J* = 6.6 Hz, 2H, C***H***=CH$_2$, C***H'***=CH$_2$), 5.26 (d, *J* = 3.5 Hz, 1H, ***H***1α), 5.09 (t, *J* = 12.3 Hz, 2H, CH=C***H***$_2$, CH=C***H'***$_2$), 5.03 (d, *J* = 10.2 Hz, 2H, CH=C***H***$_2$, CH=C***H'***$_2$), 4.58 (d, *J* = 7.8 Hz, 1H, ***H***1β), 4.24 – 4.18 (m, 1H, ***H***5'), 3.97 (s, 1H, ***H***5), 3.92 (d, *J* = 3.1 Hz, 1H, ***H***4), 3.86 (dd, *J* = 10.6 Hz, *J* = 3.1 Hz, 1H, ***H***3'), 3.81 (dd, *J* = 9.5 Hz, *J* = 4.3 Hz, 1H, ***H***2'), 3.69 (t, *J* = 5.5 Hz, 2H, ***H***6a,b), 3.67 – 3.62 (m, 1H, ***H***3), 3.62 – 3.54 (m, 2H, OC***H***$_2$), 3.53 – 3.46 (m, 1H, ***H***2), 2.13 (dd, *J* = 13.9 Hz, *J* = 6.9 Hz, 4H, C***H***$_2$CH=CH$_2$, C***H'***$_2$CH=CH$_2$), 1.76 – 1.65 (m, 4H, OCH$_2$C***H***$_2$, OCH$_2$C***H'***$_2$) ppm.

^{13}C-NMR (101 MHz, D_2O): δ = 138.8 (***C***H=CH_2), 114.7 (CH=***C***H_2), 96.4 (***C***1β), 92.3 (***C***1α), 73.3 (***C***2'), 72.7 (***C***3), 71.8 (***C***2), 70.8 (O***C***H_2), 69.7 (***C***6), 69.6 (***C***5), 69.1 (***C***3'), 69.0 (***C***4), 68.6 (***C***5), 29.5 (***C***H_2CH=CH_2), 27.7 (OCH_2***C***H_2) ppm.

2.2. Kinetic Studies

The kinetic studies were performed in aqueous PBS buffer at pH = 7.4 as solvent. The reaction progress was monitored by following the decrease in tetrazine absorption at 530 nm. The optimal tetrazine concentration was determined by an absorbance screen, determining a concentration of 0.6 mM 6-methyl-tetrzaine-amine as optimal concentration per well. A stock solution of 20 mM was prepared of every de-acetylated galactose derivative, from which further dilutions of 16 mM, 12 mM, 8 mM and 4 mM were prepared. The solutions of galactose derivatives and 6-methyl-tetrazine-amine were mixed to a final volume of 100 µL in 96-well plates and the decline in absorption at 530 nm was followed for 16 h in a microplate reader at 37 °C. The pseudo-first order rate constant k_{obs} was calculated for each concentration using GraphPad Prism 6.01 with an exponential decay function. The corresponding second order rate constant k_2 for each galactose derivative was calculated based on the concentration dependent values for k_{obs} and the resulting linear function.

2.3. Cell Culture

All cell lines were maintained in a humidified incubator at 37°C under 5% CO_2 and split before reaching confluence using TrypLE™ Express. All cell lines were grown in DMEM medium (high glucose) supplemented with 10% heat-inactivated FBS, 2 mM GlutaMAX™, 10 mM HEPES, 1% NEAA, 100 units/mL penicillin and 100 µg/mL streptomycine, further named complete medium (cDMEM). All reagents were bought from Gibco, Life Technologies (USA).

2.3.1. Cell toxicity

The toxicity of the galactose derivatives was assessed using a CellTiter-Blue^{R} Cell Viability Assay (Promega, USA). In this approach the conversion of the dye reaszurine into the fluorescent resorufin product by metabolically active cells is measured. Cells were seeded at a concentration of 10000 cells/ well (100 µl) for 48 h or 5000 cells/well (100 µl) for 72 h timepoints in a flat-bottom 96 well-plate and allowed to adhere and adapt to the plates for 24 h. After this, the cell culture medium was exchanged to complete medium supplemented with 100 µM or 200 µM of the corresponding galactose derivative. Each concentration was assed in technical triplicates. Plates were incubated for 48 h or 72 h after which the cell viability was determined by exchanging the culture medium to medium supplemented with CellTiter-Blue Reagent (dilution 1:20 from commercial stock). The plates were incubated for additional 1 h 30 min with the reagent, before analyzing the fluorescence intensity on a Infinite M200 (Tecan, USA) plate reader (λ_{exc} = 530, λ_{em} = 590). Relative fluorescence units were normalized to the values obtained for the appropriate vehicle controls and the results were shown as a percentage of the values obtained from cells cultured with the vehicle.

2.3.2. Metabolic Labeling in Huh7 and HepG2 cells

Cells were seeded with a density of 15000 cells/well (300 µL) on glass coverslips in 24-well plates and allowed to adhere for 24 h. Following this, the cell culture medium was exchanged to complete medium supplemented with 100 µM of the corresponding galactose derivative and the cells were cultured for 72 h. After this, the medium was removed and complete medium containing 25 µg/mL streptavidine (from 1 mg/mL stock in water) was added for 40 min to block endogenous biotin. The solution was aspirated and the cells were washed with PBS (3x, 200 µL/well). The labeling reaction was performed adding complete medium containing 200 µM 6-methyl-tetrazine-peg4-biotin (Jena Bioscience, stock of 1.5 mM in DMSO) to the cells and allow the reaction to occure for 5 h at 37 °C in the incubator. The tetrazine containing media was removed and the cells were washed with PBS (3x, 200 µL/well), followed by adding 6.6 µg/mL Alexa-Fluor-568-streptavidine (in PBS + 5% FBS, 200 µL/well, 20 min, RT) and Hoechst 33342 (in PBS + 5% FBS, 1:1000, 5 min, RT). For labeling of the cell membrane, CellMask ^{TM} Deep Red Plasma membrane stain (ThermoFisher scientific, in PBS + 5% FBS, 1:1000, 2 min, 37 °C) was applied before proceeding with the fixation protocol.

The cells were fixed using 4% PFA solution for 10 min at RT and the coverslips were mounted on glass objective slides using Fluoromount G™. The cells were analyzed using a LSM880 confocal point-scanning microscope (Zeiss, Germany), equipped with a Diode 405-30 nm (Hoechst) and a DPSS 561-20 nm (Alexa-Fluor-568) laser unit. The pictures were acquired with a 63x Plan-Apochromat Oil objective and processed with ImageJ 1.49v software to remove background noise. Representative images were chosen from 5 different experiments. Quantification of the fluorescence intensity resulting from the incorporated galactose derivatives and labeling with 6-methyl-tetrazine-peg4-biotin and Alexa-Fluor-568-streptavidine was done using ImageJ 1.49v software by selecting the individual cells per picture as region of interest and comparing the intensity. The values were presented as ratio to the intensity of the corresponding negative control.

The labeling experiments were performed in the same way using acetyl protected galactose derivatives or deprotected derivatives.

2.3.3. Metabolic labeling of HepG2 cells in presence of inhibitors for GLUT1

HepG2 cells were seeded in 24-well plates, either on glass coverslips (15000/well) for microscopy analysis or on the plain plate (50000/well) for analysis by flow cytometry. The cells were allowed to adhere for 24h, before the medium was changed to complete medium containing 100 µM of the unnatural galactose derivative and different concentrations of the inhibitor (10 µM of WZB117, STF31 and cytochalasine B for microscopy studies; 10 µM, 20 µM and 30 µM of WZB117 for flow cytometry). The stock solutions of all inhibitors were prepared in DMSO at a concentration of 20 mM for WZB117 and STF31, as well as 2 mM for Cytochalasine B. The cells were grown for 72 h in the presence of the unnatural galactose derivative and the inhibitors, before being analyzed by confocal point scanning microscopy or flow cytometry.

For microscopy analysis, the medium was removed and complete medium containing 25 µg/mL streptavidine (from 1 mg/mL stock in water) was added for 40 min to block endogenous biotin. The solution was aspirated and the cells were washed with PBS (3x, 200 µL/well). The labeling reaction was performed adding complete medium containing 200 µM 6-methyl-tetrazine-peg4-biotin (Jena Bioscience, stock of 1.5 mM in DMSO) to the cells and allow the reaction to occure for 5 h at 37 °C in the incubator. The tetrazine containing media was removed

and the cells were washed with PBS (3x, 200 µL/well), followed by adding 6.6 µg/mL Alexa-Fluor-568-streptavidine (in PBS + 5% FBS, 200 µL/well, 20 min, RT) and Hoechst 33342 (in PBS + 5% FBS, 1:1000, 5 min, RT). The cells were fixed using 4% PFA solution for 10 min at RT and the coverslips were mounted on glass objective slides using Fluoromount G™. The cells were analyzed using a LSM880 confocal point-scanning microscope (Zeiss, Germany), equipped with a Diode 405-30 nm (Hoechst) and a DPSS 561-20 nm (Alexa-Fluor-568) laser unit. The pictures were acquired with a 63x Plan-Apochromat Oil objective and processed with ImageJ 1.49v software to remove background noise and quantify the mean fluorescence intensity per cell of the sugar derived labeling.

For analysis by flow cytometry, the medium was aspirated after 72 h and complete medium containing 25 µg/mL streptavidin (from 1 mg/mL stock in water) was added for 40 min at 37 °C to block endogenous biotin. The cells were rinsed with PBS (3 x 200 µL/well) and complete medium containing 200 µM 6-methyl-tetrazine-peg4-biotin was added for 5 h at 37 °C. The medium was removed and the cells were detached with 20 mM EDTA solution (5 min, 37°C), collected by centrifugation (2000 g, 5 min) and washed with PBS + 5% FBS (100 µl per cell pellet). 6.6 µg/mL Alexa-Fluor-568-streptavidin in PBS + 5% FBS (100 µL per cell pellet) was added for 20 min at RT, followed by washing the cell pellet with PBS + 5% FBS (3x100 µL per cell pellet). The cells were fixed with 4% PFA solution (8 min, RT) and resuspended in 300 µL PBS + 5% FBS for analysis. The cells were analyzed in a BD LSRFortessa X-20 cell analyzer, using a 561 nm laser (Alexa-Fluor-568). The results were analyzed using FACSDiva, FLOWJOW and GraphPad Prism software packages.

2.3.4. Metabolic labeling of HepG2 cells for cell lysis and pull-down

HepG2 cells were seeded in T75 flasks (1.5*106 cells/flask) in DMEM medium (high glucose), supplemented with 10% heat-inactivated FBS, 1% GlutaMAX, 1% HEPES, 1% NEAA and 100 units/mL penicillin and streptomycine, further named complete medium (cDMEM). The cells were allowed to attache at least 12 h, before the medium was changed to cDMEM supplemented with 100 µM penta-acetyl-galactose (Ac5Gal), 1,3,4,6-tetraacetyl-2-O pentenyl-galactose (2OPent) or 1,2,3,4-tetraacetyl-6 O pentenyl-galactose (6OPent). The cells were grown for 72 h, before the

media was removed and the cells were gently flushed with PBS (1x). The cells were harvested using 1 mL of lysis buffer (20 mM Tris pH = 7.6, 300 mM NaCl, 1% TritonX100, 5% glycerol, 1 mM EDTA, 1:10 protease inhibitor) and incubated on ice for 30 min. The cell lysate was obtained after centrifugation at 14000 g for 10 min at 4°C. 200 µL of whole cell lysate were treated with 50 µM of 6 methyl tetrazine peg4 bioting and the labelling reaction was performed at room temperature overnight. To each sample, 100 µl of a suspension of streptavidin magnetic beads (Pierce Streptavidin Magnetic Beads, 10 mg/mL) was added and the binding was performed at room temperature for 1 h. The supernatant was collected and the magnetic beads were washed twice with PBS (1x). The magnetic beads were suspended in 50 µL 4xSDS loading buffer with 100 µM DTT and boiled for 10 min at 90 °C. The samples were resolved in a 12% SDS gel.

2.3.5. Competition experiment and Inhibition of *O*-glycosylation

HepG2 cells were seeded on glass coverslips in 24-well plates (15000 cells/well) and were allowed to attach. On the next day, the media was changed to cDMEM supplemented with an indicated concentration of **2b**, **5** or **9**. For competition experiments the same concentration of **9** was added to samples with **2b**. For an inhibition of *O*-glycosylation, Benzyl 2-acetamido-2-deoxy-α-d-galactopyranoside (BADG) was added with 100 µM after 24 h of cell growth until the end of a total culturing time of 72 h. After a culturing time of 72 h, the media was removed and endogenous biotin was blocked with 25 µg/mL streptavidin (in 200 µL cDMEM, 30 min @ 37 °C). The samples were washed repeatedly with PBS, before a solution of 200 µM 6-methyl--tetrazine-peg4-biotin in 200 µL cDMEM was added (5 h @ 37 °C). The media was removed and the cells were rinsed with PBS. The staining was performed with 6.6 µg/mL Alexa-Fluor-568-streptavidin in PBS + 3% FBS (30 min @ room temperature) and Hoechst 33342 (1:1000, 8 min @ room temperature). The cells were fixed with 4% paraformaldehyde solution (8 min @ room temperature) and mounted on glass objectives with Fluoromount G™. The pictures were acquired on a LSM880 confocal point-scanning microscope (Zeiss, Germany), equipped with a Diode 405-30 nm (Hoechst) and a DPSS 562-20 nm (Alexa-Fluor-568) laser unit. A 63x Plan-Apochromat Oil objective was used for acquisition and the pictures were analysed by using ImageJ 1.49v software package. Pictures were acquired from different regions on the coverslips and the

fluorescence intensity resulting from incorporated galactose derivatives was quantified by assigning ROIs to single cells.

2.3.6. Release of cell surface glycans

Huh7 cells were seeded in 6-well plates (1x106 cells/ well) in cDMEM and were allowed to attach overnight. On the next day, the media was changed to cDMEM supplemented with 100 µM of **9** or **2b** and the cells were cultured for 72 h. To analyse possible cell surface glycans, the cells were harvested in cDMEM and washed with 500 µL PBS (3x, 600 rpm, 10 min @ 4 °C). The cells were suspended in 500 µL PBS and 10 µL of Trypsin solution (20 µg trypsin in 100 µL acetic acid 50 mM) was added. The reaction was incubated at 37 °C for 15 min, before the supernatant was separated (15000 rpm, 15 min @ 4 °C). The supernatant was collected and trypsin was heat-inactivated @ 98°C for 5 min.

A 5 µL sample of the supernatant was diluted with 5 µL MilliQ water and the reaction was performed with 1 µL 6-Methyl-tetrazine-sulfo-Cy3 solution (1.1 mM in PBS) overnight @ 37 °C. A sample of 1 µL was diluted with 9 µL MilliQ water for analysis in an Acquity LC/MS system.

It was possible to detect a specific peak at 553nm in cells treated with compound **2b** for 72 h.

2.4. Infection Studies

Sporozoites from *Plasmodium berghei*, expressing green fluorescent protein (GFP), were dissected in non-supplemented DMEM medium from the salivary glands of infected female *A. stephensi* mosquitoes, bred at Instituto de Medicina Molecular. In general, HepG2 cells were seeded one day prior to infection to adhere in the cell culture plates.

2.4.1. Infection of HepG2 cells and analysis by confocal microscopy

HepG2 cells were seeded on glass coverslips (15000/well, 300 µL) in 24-well plates and allowed to adhere for 24h in complete medium. On the day of infection, the medium was aspirated and exchanged to complete medium supplemented with 100 µM of the corresponding galactose derivative (from 100 mM stock in DMSO) or the control sugar and Fungizone (1:200, from commercial stock). GFP-expressing sporozoites from *Plasmodium berghei* were dissected in DMEM from salivary glands of infected female *A. stephensi* mosquitoes and 60000 sporozoites per well were added directly to the cells. The plate was centrifuged for 4 min at 200g to ensure simultaneous settling of the sporozoites on the cells. After 2 hpi, the medium was removed carefully and the cells were rinsed with PBS (3x 200 µL/well) to remove mosquito host debris, before adding again complete medium containing 100 µm of the galactose derivative or the control sugar and fungizone. The cells were grown in a humidified incubator at 37 °C with 5% CO_2 until 48 hpi. At this point, the same staining procedure as described in the section above was applied to the cells and the fluorescence intensity resulting from the incorporation of the unnatural galactose derivatives was analyzed in a LSM880 confocal point-scanning microscope (Zeiss, Germany), equipped with a Diode 405-30 nm (Hoechst) and a DPSS 561-20 nm (Alexa-Fluor-568) laser unit. The pictures were acquired with a 63x Plan-Apochromat Oil objective and processed with ImageJ 1.49v software to remove background noise. Representative images were chosen from 5 different experiments. Quantification of the fluorescence intensity resulting from the incorporated galactose derivatives and labeling with 6-methyl-tetrazine-peg4-biotin and Alexa-Fluor-568-streptavidine was done using ImageJ 1.49v software by selecting the individual cells per picture as region of interest and comparing the intensity. The values were presented as ratio to the intensity of the corresponding negative control.

2.4.2. Infection of HepG2 cells and analysis by flow cytometry and imaging flow cytometry

HepG2 cells were seeded (50000/well, 300 µL) in 24-well plates and allowed to adhere for 24h in complete medium. On the day of infection, the medium was aspirated and exchanged to complete medium supplemented with 100 µM of the corresponding galactose derivative (from 100 mM stock in DMSO) or the control sugar and Fungizone (1:200, from commercial stock). GFP-expressing sporozoites from *Plasmodium berghei* were dissected in DMEM from salivary glands of infected

female *A. stephensi* mosquitoes and 60000 sporozoites per well were added directly to the cells. The plate was centrifuged for 4 min at 200g to ensure simultaneous settling of the sporozoites on the cells. After 2 hpi, the medium was removed carefully and the cells were rinsed with PBS (3x 200 µL/well) to remove mosquito host debris, before adding again complete medium containing 100 µm of the galactose derivative or the control sugar and fungizone. The cells were grown in a humidified incubator at 37 °C with 5% CO_2 until 48 hpi. The medium was aspirated and complete medium containing 25 µg/mL streptavidine (from 1 mg/mL stock in water) was added for 40 min at 37 °C to block endogenous biotin. The cells were rinsed with PBS (3 x 200 µL/well) and complete medium containing 200 µM 6-methyl-tetrazine-peg4-biotin was added for 5 h at 37 °C. The medium was removed and the cells were detached with 20 mM EDTA solution (5 min, 37°C), collected by centrifugation (2000 g, 5 min) and washed with PBS + 5% FBS (100 µl per cell pellet). 6.6 µg/mL Alexa-Fluor-568-streptavidin in PBS + 5% FBS (100 µL per cell pellet) was added for 20 min at RT, followed by washing the cell pellet with PBS + 5% FBS (3x100 µL per cell pellet). The cells were fixed with 4% PFA solution (8 min, RT) and resuspended in 300 µL PBS + 5% FBS for analysis. The cells were analyzed in a BD LSRFortessa X-20 cell analyzer, using a 488 nm laser (GFP) and 561 nm laser (Alexa-Fluor-568). The results were analyzed using FACSDiva, FLOWJOW and GraphPad Prism software packages. The data shown result from a pool of at least 3 different experiments. The mean or median fluorescence intensities resulting from the incorporated unnatural galactose derivative (Alexa-Fluor-568) were presented as ratio to the corresponding negative control.

For analysis using Amnis ImageStreamX imaging flow cytometer, the cells were grown, infected and stained in the same way as described above. The final volume of the cells in PBS + 5% FBS was decreased to 100 µL. A 488nm laser (GFP) and 561 nm laser (Alexa-Fluor-568) were used for the analysis, as well as bright field light. A typical acquisition setting is represented below, starting from the gating on single cells based on their bright field aspect ratio intensity and area. These single cells were restricted to those being in the focus of the camera, followed by distinguishing between non-infected and infected cells based on the intensity of the GFP signal. Finally, the mean and median fluorescence intensity resulting from the incorporated galactose derivative (Alexa-Fluor-568) was analyzed and represented as a ratio to the corresponding control. The presented data result from as a pool from two individual experiments which were performed with technical duplicates.

3. NMR Spectra

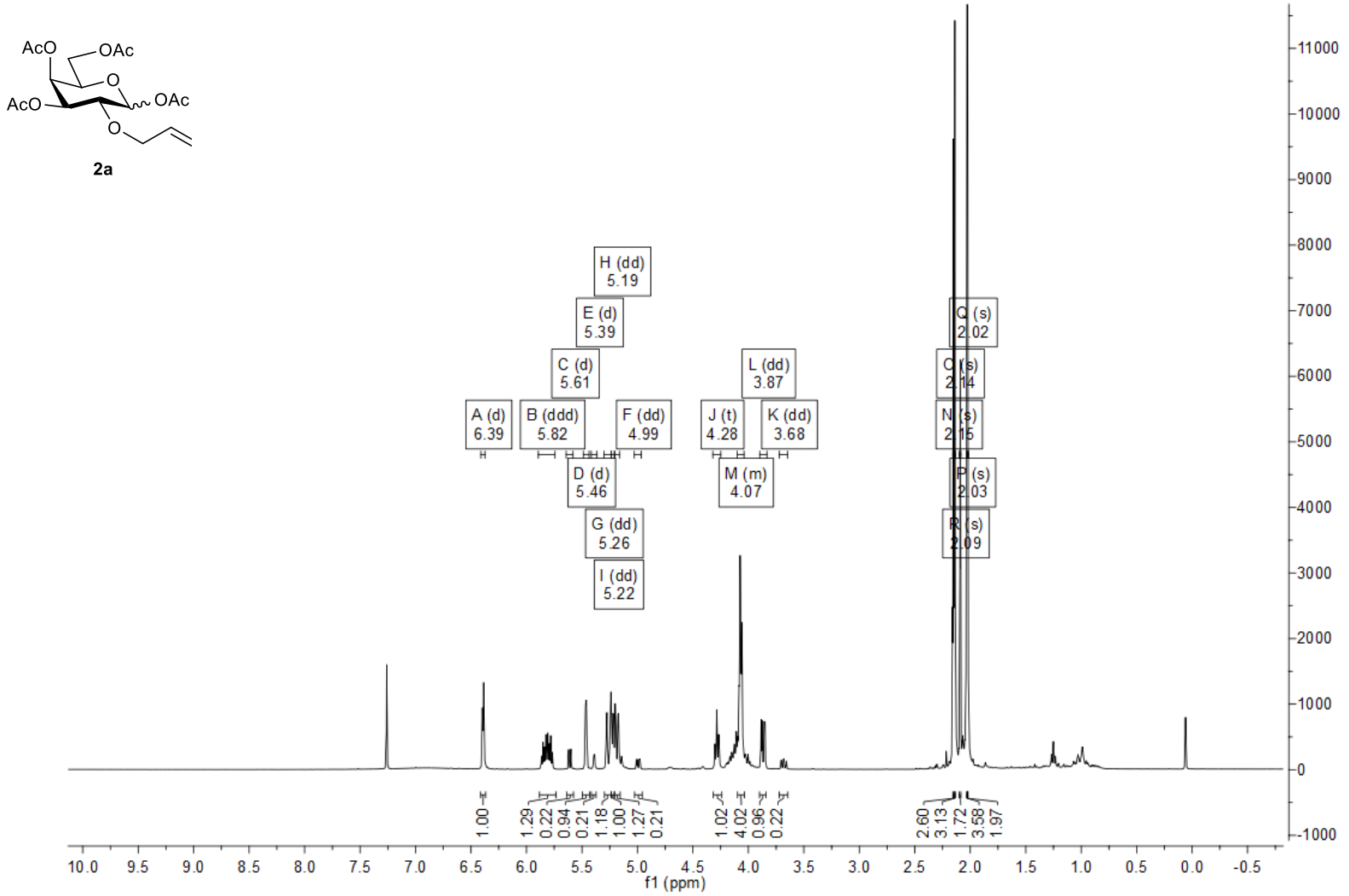

Figure S15: ^{1}H NMR of **2a** ($CDCl_3$, 400 MHz).

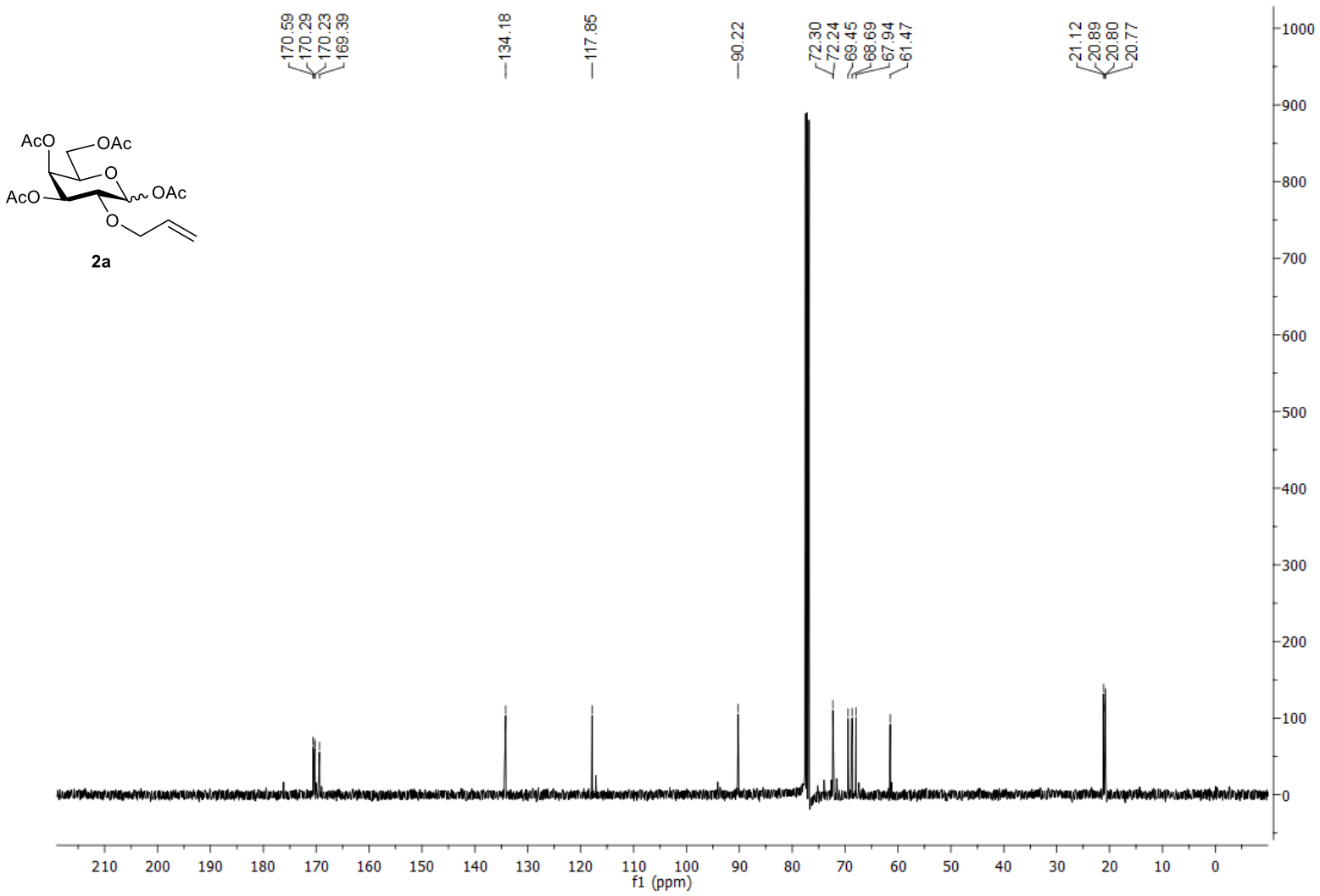

Figure S16: ^{13}C NMR of **2a** ($CDCl_3$, 100 MHz).

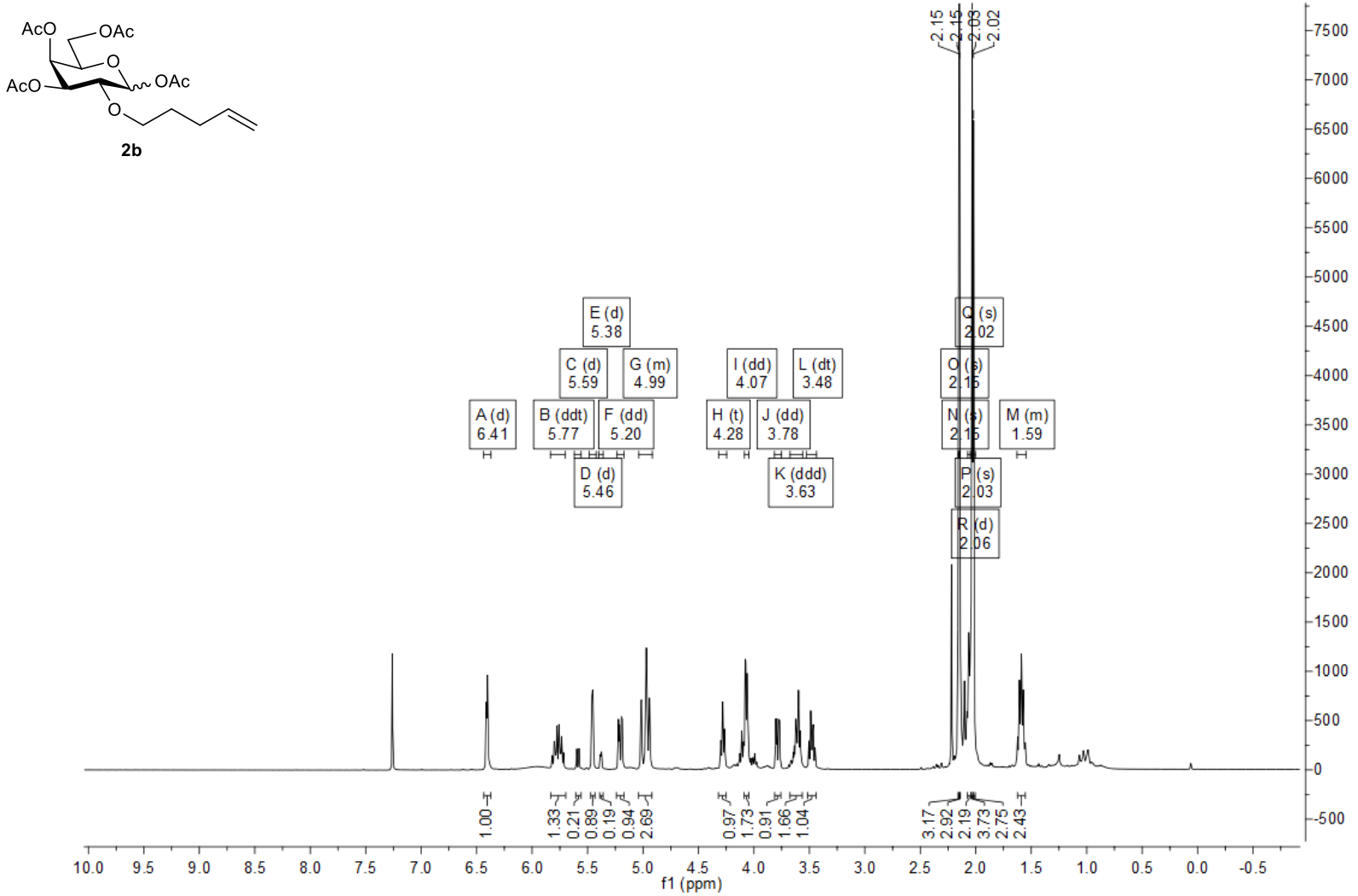

Figure S17: ^{1}H NMR of **2b** ($CDCl_3$, 400 MHz).

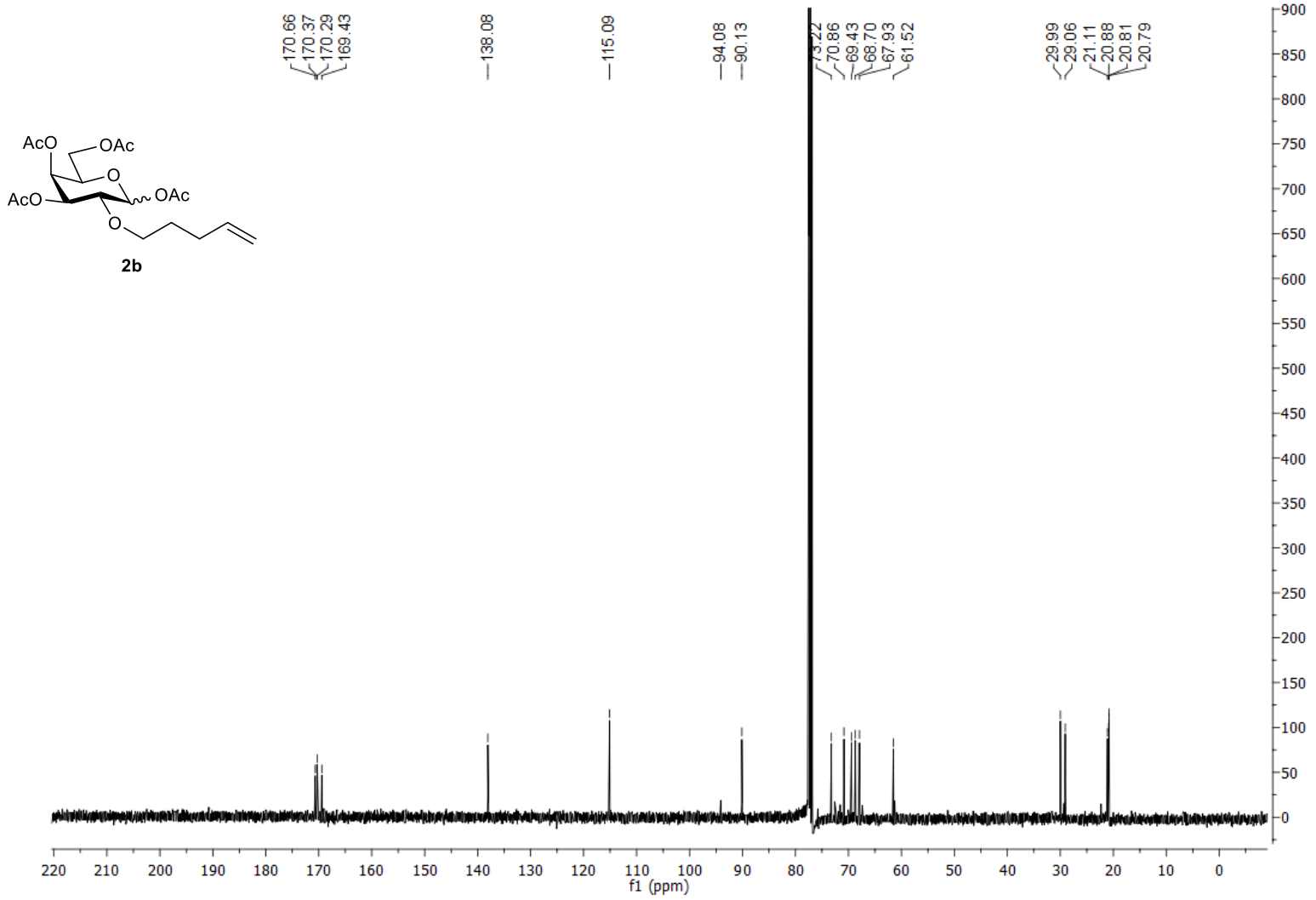

Figure S18: ^{13}C NMR of **2b** ($CDCl_3$, 100 MHz).

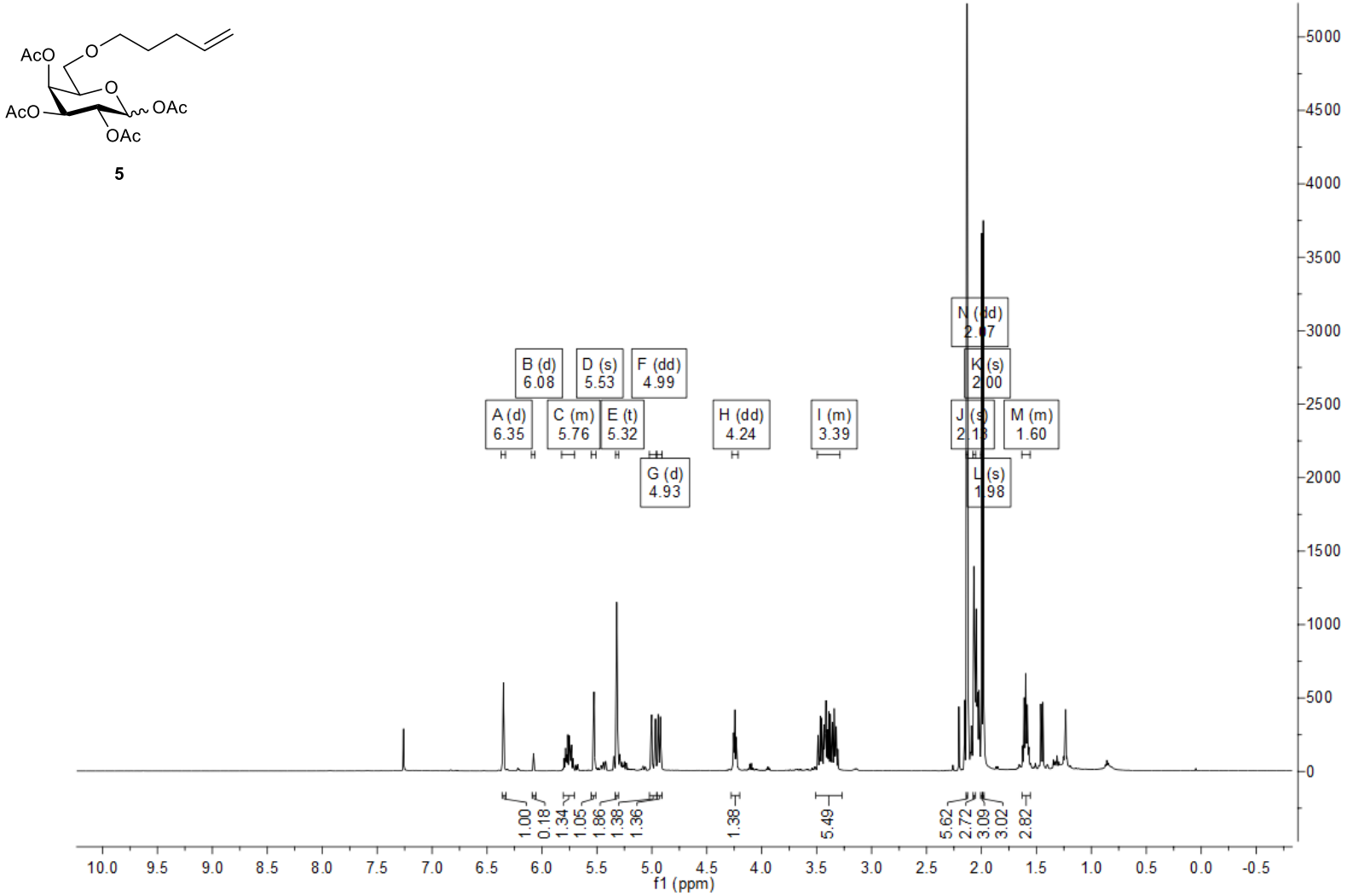

Figure S19: ^{1}H NMR of **5** ($CDCl_3$, 400 MHz).

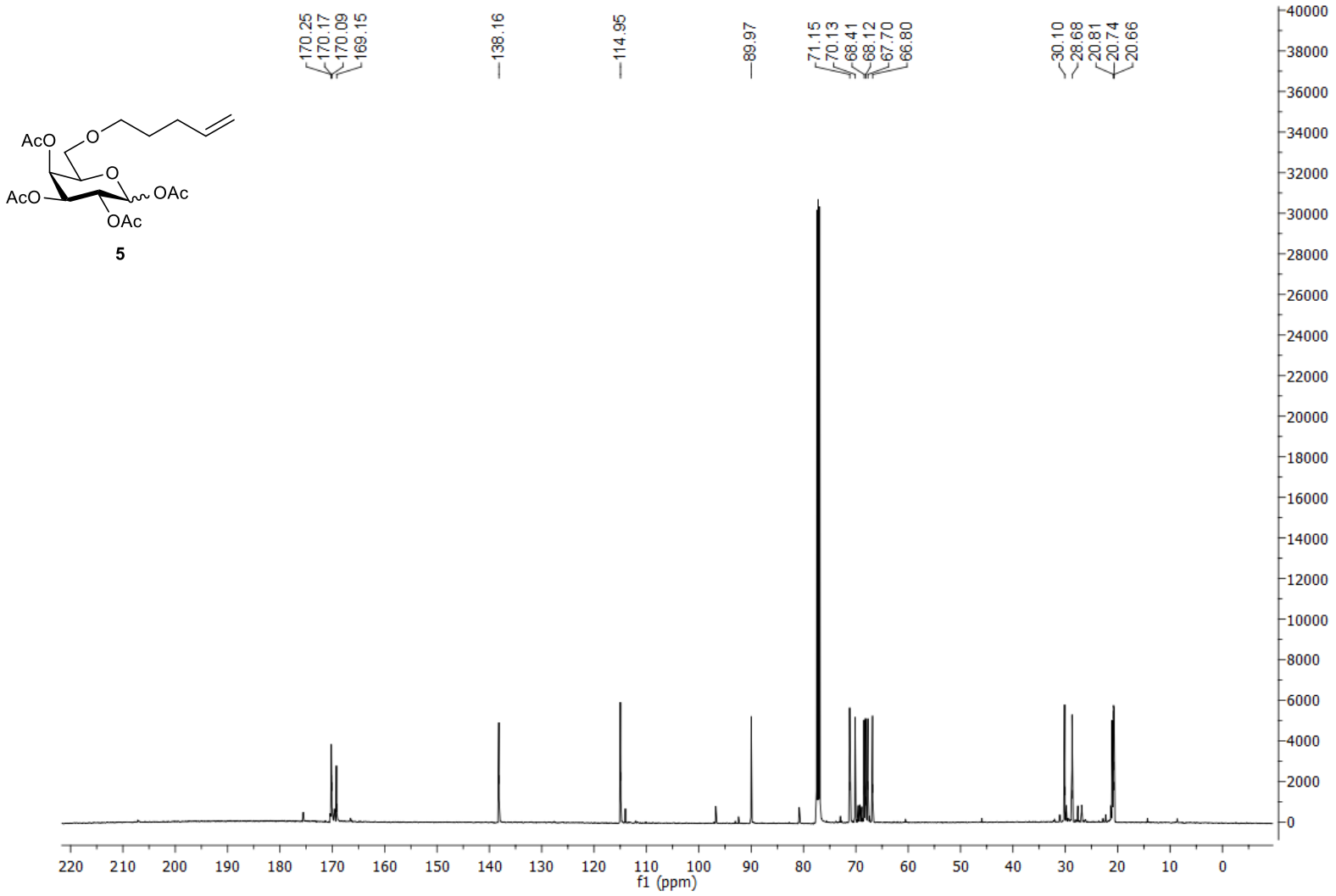

Figure S20: ^{13}C NMR of **5** ($CDCl_3$, 126 MHz).

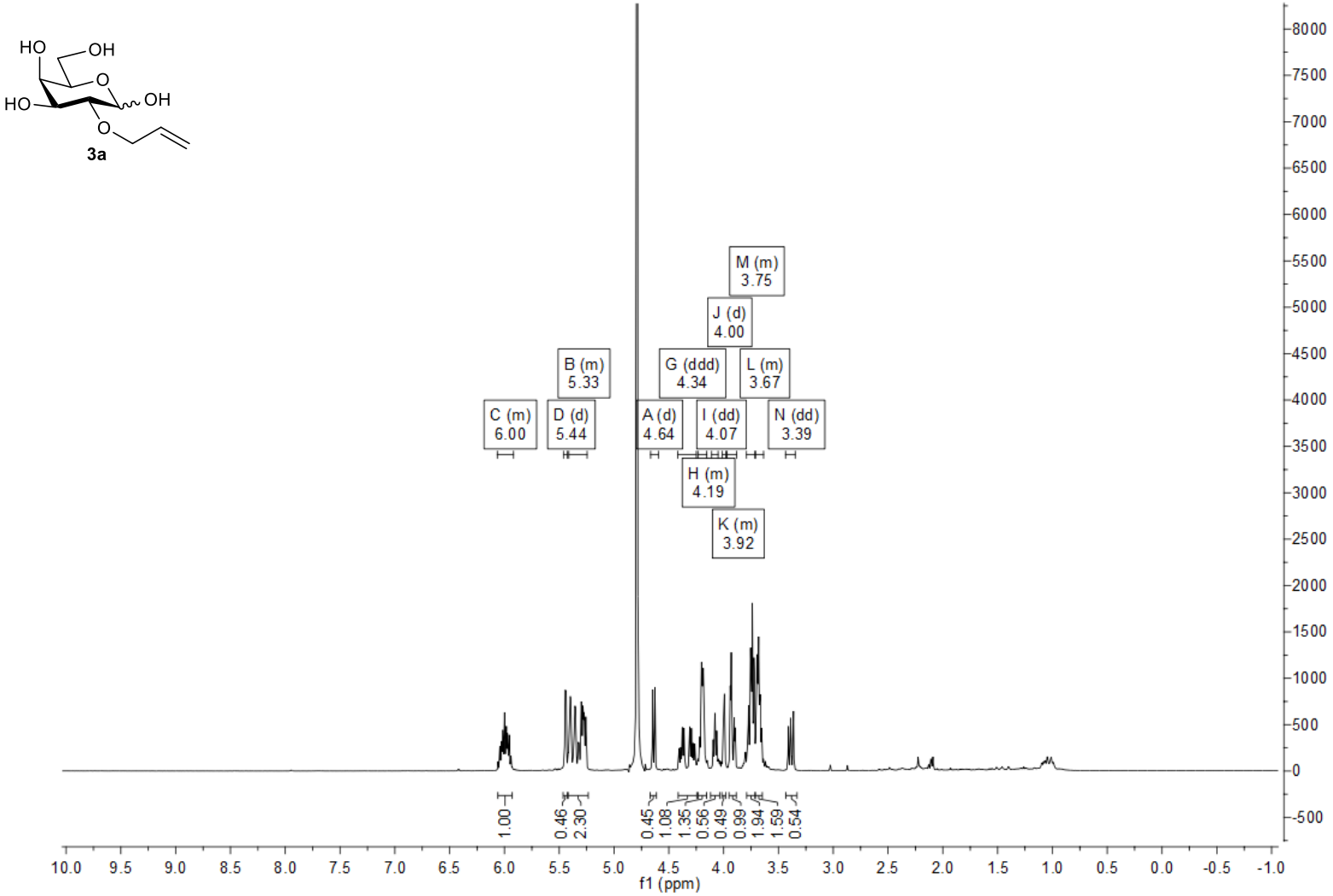

Figure S21: ^{1}H NMR of **3a** (D_2O, 400 MHz).

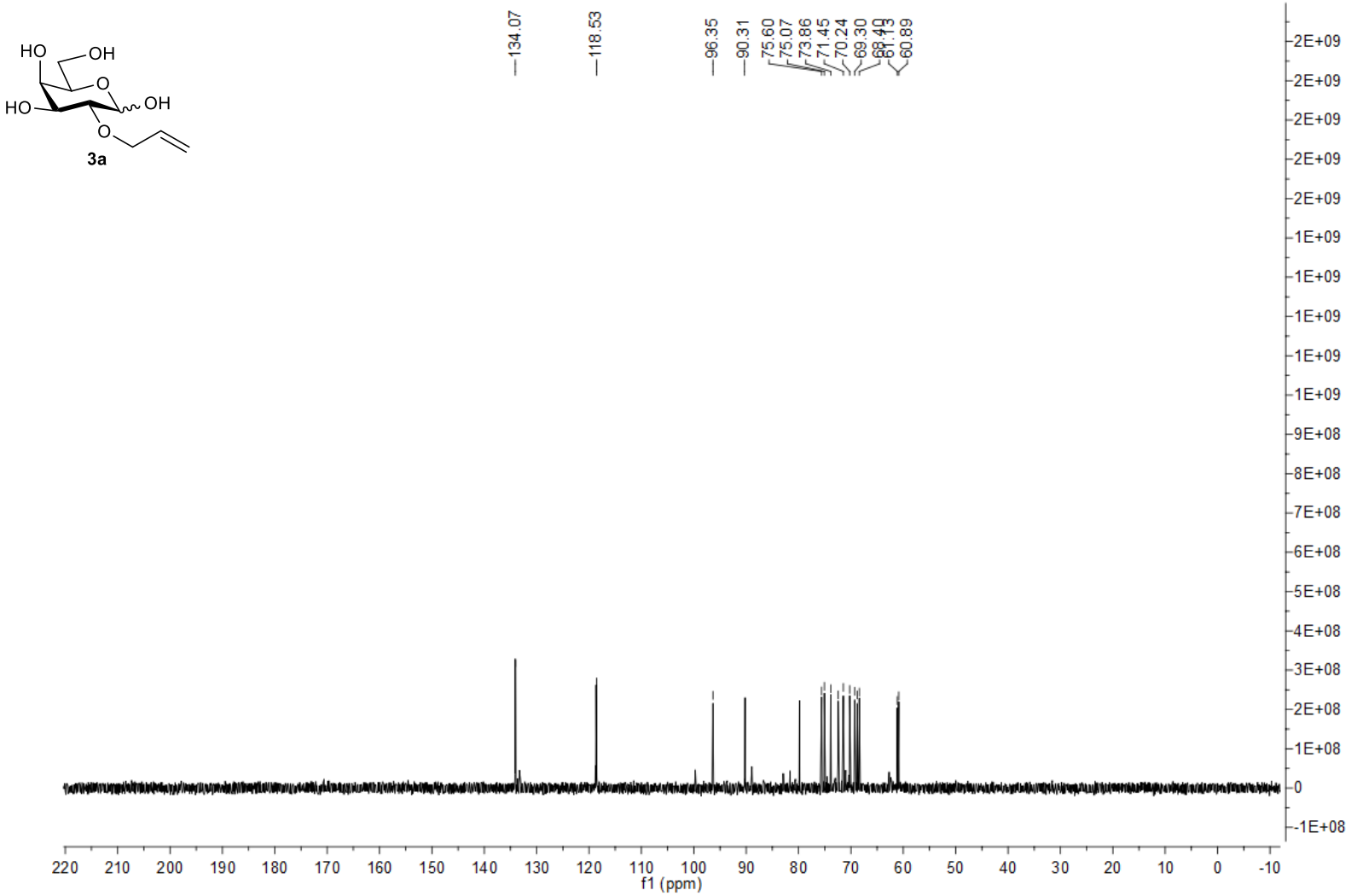

Figure S22: ^{13}C NMR of **3a** (D_2O, 100 MHz).

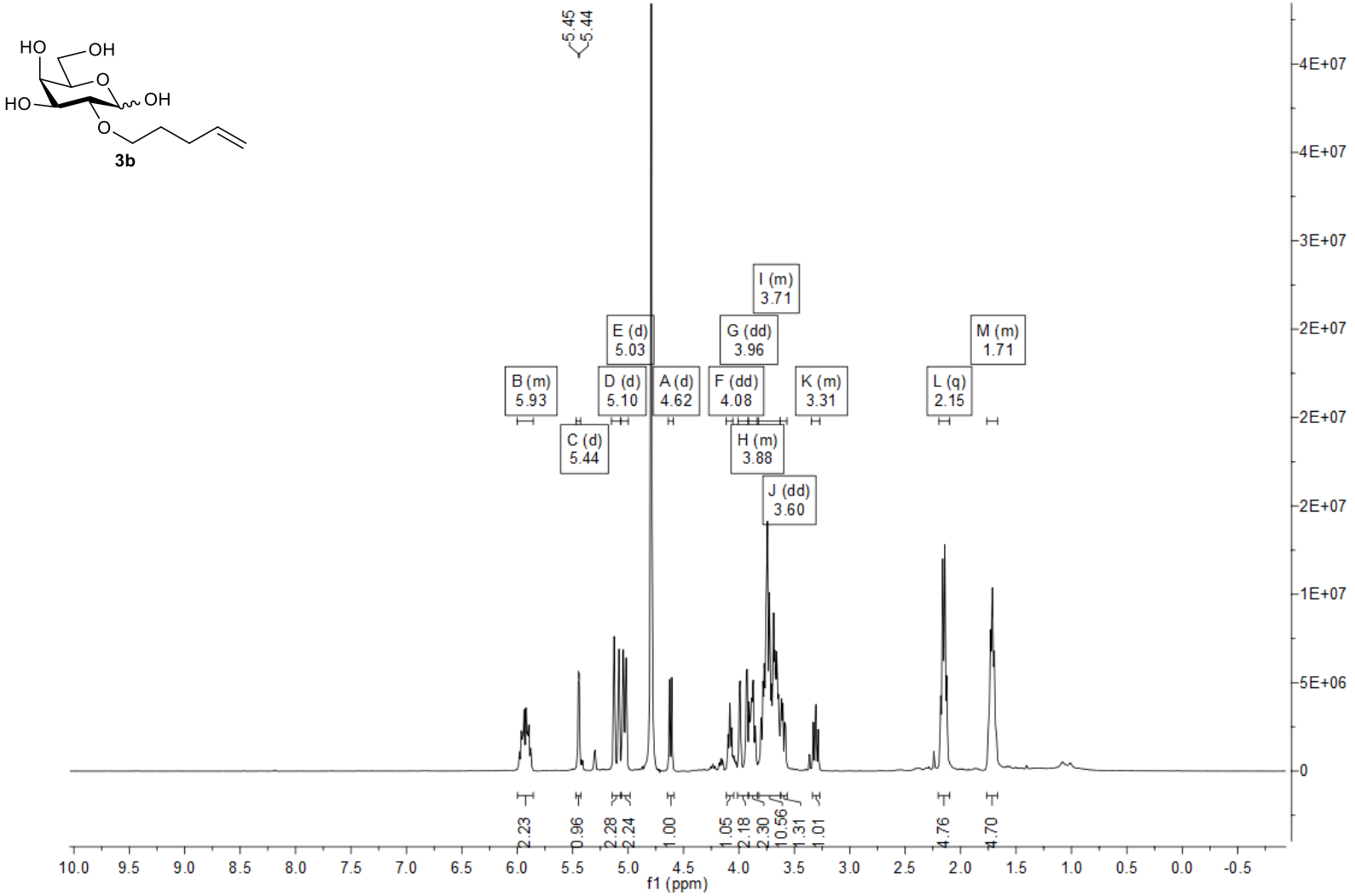

Figure S23: ^{1}H NMR of **3b** (D_2O, 400 MHz).

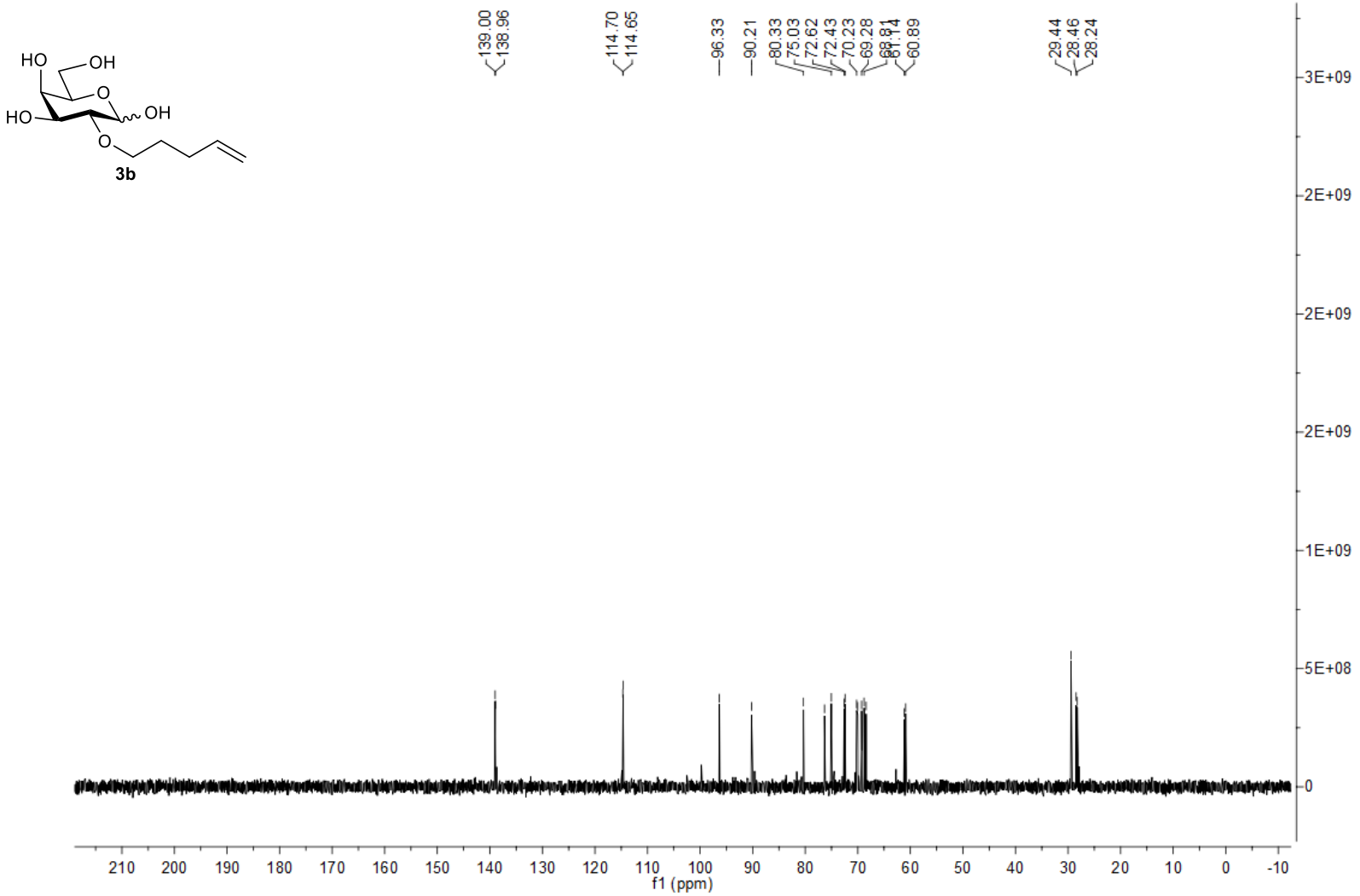

Figure S24: ^{13}C NMR of **3b** (D_2O, 100 MHz).

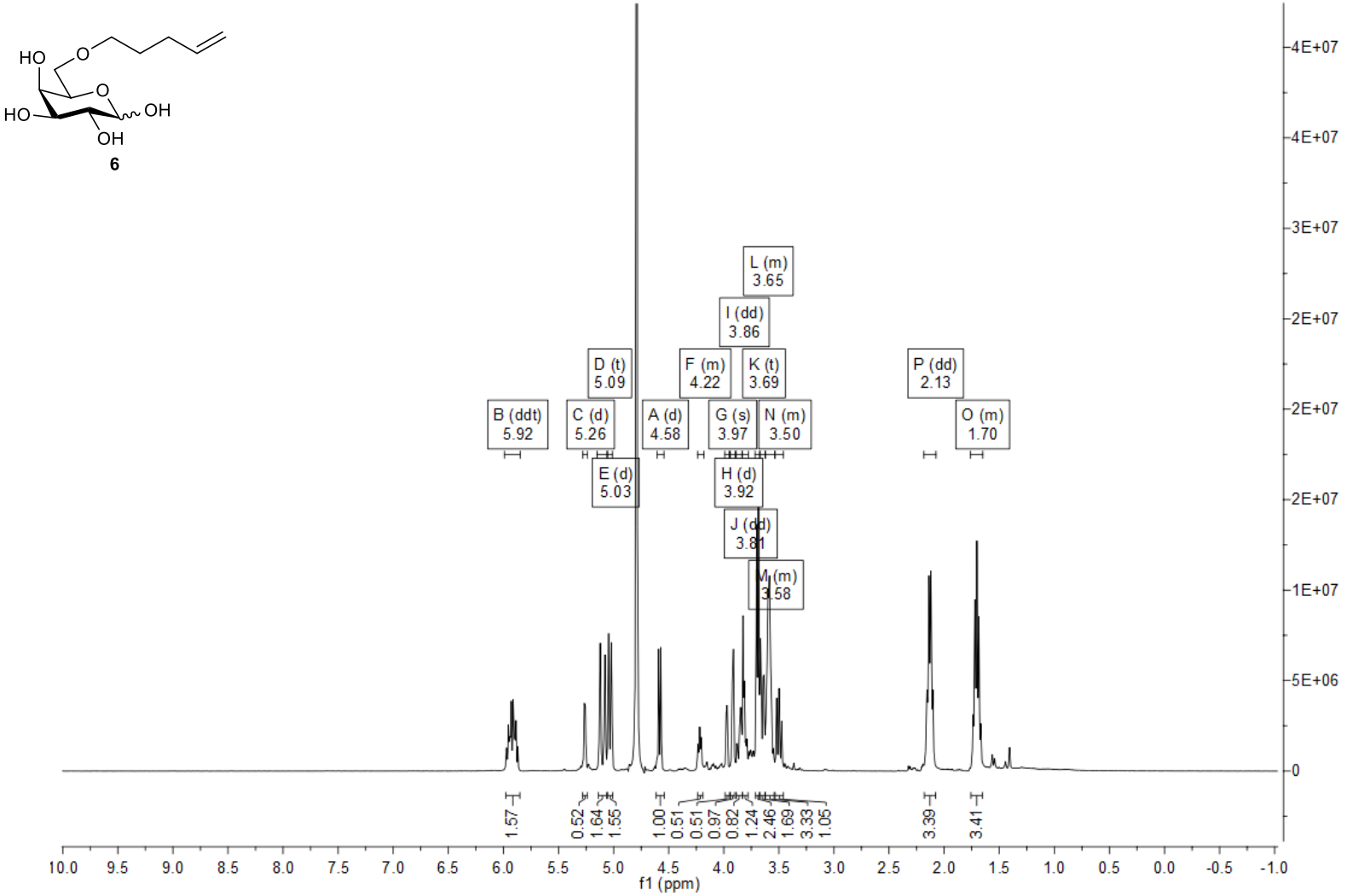

Figure S25: ^{1}H NMR of **6** (D_2O, 400 MHz).

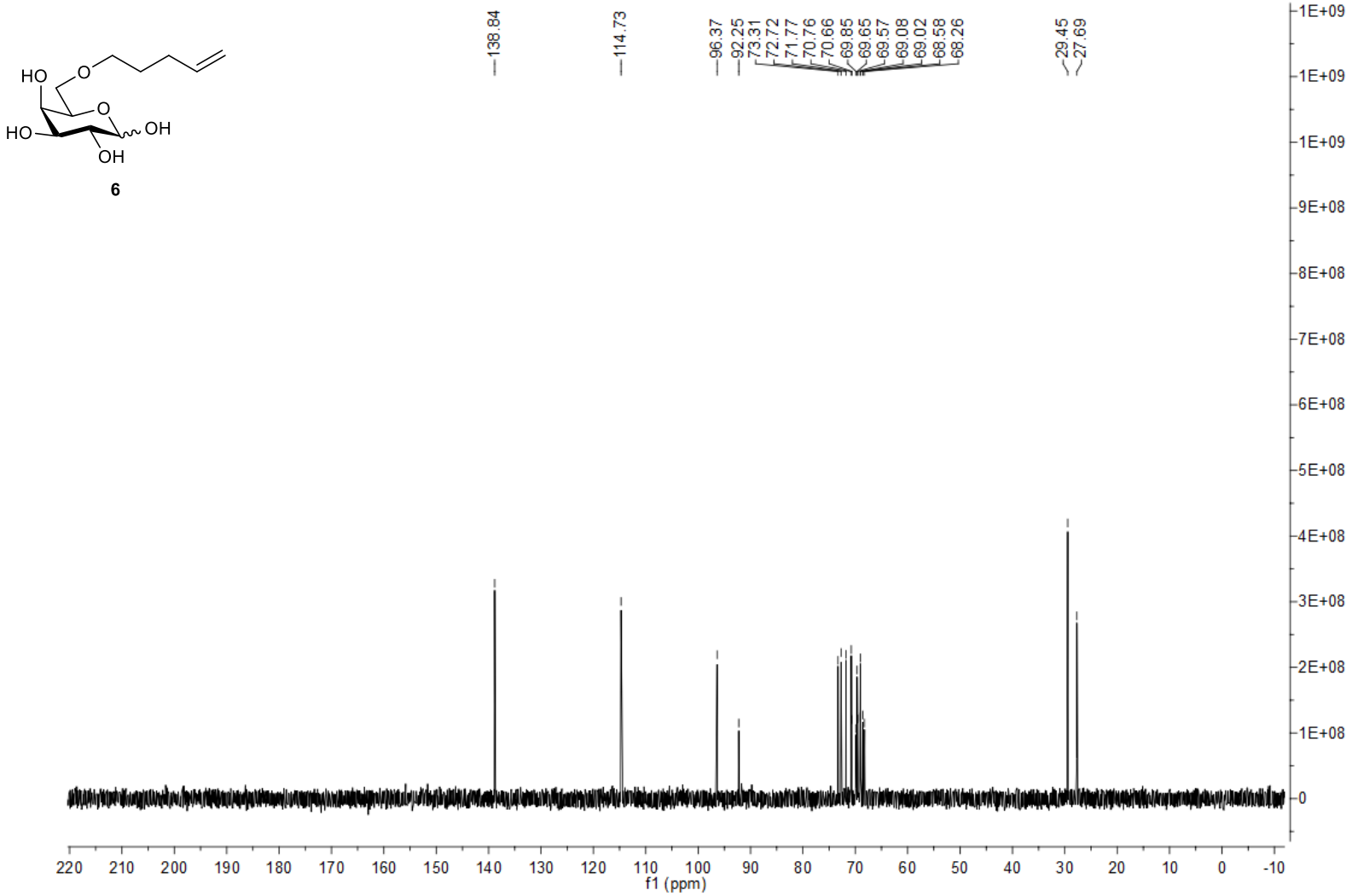

Figure S26: ^{13}C NMR of **6** (D_2O, 100 MHz).